

**Random Quantum Dynamics:
From Random Quantum Circuits to Quantum Chaos**

A Thesis

Submitted to the Faculty

in partial fulfillment of the requirements for the

degree of

Doctor of Philosophy

in

Physics and Astronomy

by

Winton G. Brown

DARTMOUTH COLLEGE

Hanover, New Hampshire

27 October 2010

Examining Committee:

Lorenza Viola

Miles Blencowe

Chandrasekhar Ramanathan

Maxim Olshanii

Brian W. Pogue
Dean of Graduate Studies

Copyright by
Winton G. Brown
2010

Abstract

Quantum circuits consisting of single and two-qubit gates selected at random from a universal gate set are examined. Specifically, the asymptotic rate for large numbers of qubits n and large circuit depth k at which t -order statistical moments of the matrix elements of the resulting random unitary transformation converge to their values with respect to the invariant Haar measure on $U(2^n)$ are determined. The asymptotic convergence rate is obtained from the spectral gap of a superoperator describing the action of the circuit on t -copies of the system Hilbert space. For a class of random quantum circuits that are reversible and invariant under permutation of the qubit labels, the gap and hence the asymptotic convergence rate is shown to scale as $\sim 1/n$ for sufficiently large n , with a coefficient that may in general depend on t . Bounds are derived between the convergence rates for a broader class of reversible random quantum circuits and the convergence rates of second order moments of irreversible random quantum circuits are examined through a mapping to a Markov chain.

Weak constraints are constructed for finite moments of matrix elements of local observables with respect to the eigenvectors of general many-body Hamiltonians in the thermodynamic limit. This is accomplished by means of an expansion in terms of polynomials which are orthogonal with respect to the density of states. The way in which such constraints are satisfied is explored in connection to non-integrability and is argued to provide a general framework for analyzing many-body quantum chaos. Hamiltonians consisting of the XX -interaction between spin-1/2 particles (qubits) which are nearest neighbors on a 3-regular random graph (non-integrable), and an open chain (integrable), are diagonalized numerically to illustrate how the weak constraints can be satisfied. The entanglement content of the eigenvectors of chaotic many-body Hamiltonians is discussed as well as the connection between quantum chaos and thermalization in closed quantum systems.

Acknowledgements

This thesis would not have been possible without the continued encouragement and advice of my supervisor Lorenza Viola and all those who have helped me along on this path.

In particular, I would like to thank my other thesis committee members: Miles Blencowe, Chandrasekhar Ramanathan, and Maxim Olshanii for their many questions and valuable feedback. I would like to thank Yaakov Weinstein for introducing me to the problem of random quantum circuits and for numerous valuable conversations during a very fruitful collaboration. I would like to thank Lea Dos Santos for sharing with me her insight on many-body quantum chaos, without which I would not have known the right questions to ask. I would like to thank Kaveh Khodosh, Jeremy Oullette, and Paul Nation for their feedback on the many crazy ideas I have run by them. It is an honor for me to acknowledge Jay Lawrence and Robert Doyle who have given me continued guidance and encouragement since my undergraduate days. I am grateful to the staff of the physics department at Dartmouth, Judith Lowell, Bill Hamblin, Gaynell Ciccarelli, and Claudia Crosby, for assisting me in many ways.

I would never have come this far were it not for the tireless love and support of my mother Kathleen Brown. Finally, I express my profound appreciation to Rebecca Lindstrom for her enormous help in support during the writing of this thesis and throughout these last 6 years.

Contents

Abstract	ii
Acknowledgements	iii
Table of Contents	iv
List of Figures	vii
1 Introduction: Motivations and Overview	1
2 Random Quantum Circuits: Background	5
2.1 Convergence of Random Quantum Circuits	5
2.2 Tools from Harmonic Analysis	8
2.3 Convergence of Moments	10
2.3.1 Convergence Rate and Convergence Time	11
3 Reversible Random Quantum Circuits	13
3.1 Extremal State Subspace	14
3.2 Permutationally Invariant Random Quantum Circuits	17
3.2.1 Leading order coefficient	19
3.2.2 Additional invariant subspaces	20
3.3 Locally Invariant Random Quantum Circuits	21
3.3.1 Example: Haar measure on $U(4)$	24
3.4 Convergence of Random Quantum Circuits vs. Typical Gate Complexity	26

4	Irreversible Random Quantum Circuits	28
4.1	Markov Chain Reduction	29
4.2	Parallel Random Quantum Circuits and Cluster States	30
4.3	Permutationally Invariant Random Quantum Circuits	34
5	Quantum Chaos: Background	38
5.1	Eigenvalue Statistics	40
5.1.1	Bohigas-Gianonni-Schmidt conjecture	41
5.2	Eigenvector Statistics	43
5.3	Integrability and Chaos in Quantum Many-Body Systems	44
6	Constraints on the Statistical Properties of Quantum Chaotic Many-Body Hamil-	
	tonians	47
6.1	Constrains from the Thermodynamic Limit	48
6.1.1	Density of states	48
6.1.2	Microcanonical expectation values	50
6.1.3	Correlation functions	52
6.1.4	Concentration of measure and quantum ergodicity	55
6.1.4.1	Weak convergence only	55
6.1.4.2	Strong convergence only	56
6.1.4.3	Strong convergence with universal fluctuations	56
7	XX Model on Random Graphs	58
7.1	Model Hamiltonian	58
7.1.1	Symmetries	59
7.2	Eigenvalue Properties	61
7.3	Eigenvector Properties	62
7.4	Entanglement of Chaotic Eigenstates	66
7.5	Dynamics	68
8	Conclusions	70

A	Convergence Rates for Arbitrary Statistical Moments of Random Quantum Circuits	72
B	Parameters of Pseudorandom Quantum Circuits	73
C	Quantum Pseudorandomness from Cluster-State Quantum Computation	74
D	Chaos, Delocalization, and Entanglement in Disordered Heisenberg Models	75
E	Generalized Entanglement as a Framework for Complex Quantum Systems: Purity Versus Delocalization Measures	76

List of Figures

3.1	It is convenient to visualize the moment space \mathcal{H}_{M_t} as an array of 2nd qubits, with each tn qubits forming a bra and tn qubits forming a ket. The two columns, one in the bra and the other in the ket, which correspond to a single qubit determine the local moment spaces \mathcal{H}_{l_t} . The action of a two-qubit gate U is shown only to affect bi-local moment spaces $\mathcal{H}_{l_t} \otimes \mathcal{H}_{l_t}$ corresponding to the relevant qubit pair.	14
3.2	Inverse spectral gap Δ_t^{-1} of $M_t[\mu_H]$ with $t = 2, 3$ for a random circuit consisting of two-qubit gates selected according to the Haar measure on $U(4)$. The line with slope $5/6$ corresponds to the asymptotic result. From [19].	25
4.1	Schematics of cluster-state PR architectures. Pairs of qubits subjected to CZ gates are connected by solid lines and each qubit is identified by the angle in the x - y plane that defines its measurement basis. Dashed lines represent additional CZ gates for the enhanced version of the algorithm from [11].	31
4.2	Distance of the (normalized) distribution of squared moduli state-vector components from $P_{PT}(y)$ for random states as a function of run time. \square : Standard (6 rows and connections every third column), vs \circ : Enhanced (connections at every column) PR patterns. The run time equals the number of columns in the cluster state. Inset: Difference of global entanglement, Q , from the expected random-state value, Q_R , vs run time. For both test functions, the enhanced version of the algorithm converges to the Haar average with a rate about 6 times faster.	32

4.3	Gap, $\Delta(c)$, between the largest eigenvalue of 1 and the absolute value of the largest non-unit eigenvalue of $M(c)$ vs c , for $n = 6$ (solid line) and $n = 10$ (dashed line). The gap at $c = 0$ ($HZ(\alpha)$ gates) is significantly larger than the gap at $c = 1/3$ (arbitrary random single-qubit gates), identifying the optimal gate set. Inset: Gap for $c = 1/3$ (circles) and $c = 0$ (squares) vs n	34
7.1	Schematic representation of a 3-regular random graph for $n = 14$	59
7.2	Smoothed density of states $s_n(E)$ for $n = 10, 12, 14, 16$ for the subspace with $S_z = 1$	60
7.3	Empirical energy level spacing distribution $P_1(s)\delta s$ for the interval $-2 < E_\alpha < 2$ for $n = 10$ (top left), $n = 12$ (top right), $n = 14$ (bottom left) and $n = 16$ (bottom right).	61
7.4	Diagonal matrix elements $\langle \alpha h^{12} \alpha \rangle$ for the interaction term between neighboring vertices 1 and 2 in \mathcal{G} as a function of rescaled energy eigenvalues $\{E_\alpha/n\}$ with for $n = 10, 12, 14$, and 16.	62
7.5	Diagonal variance $v_D(0)$ at $\tilde{E} = 0$ for an interaction term h^{12} where 1 and 2 are neighboring vertices in \mathcal{G} as a function of n . The inverse density of states $1/s_n(0)$ evaluated at $\tilde{E} = 0$ is also given for comparison.	63
7.6	Diagonal matrix elements $\langle \alpha \sigma_z^1 \sigma_z^2 \alpha \rangle$ where 1 and 2 are neighboring vertices in \mathcal{G} as a function of rescaled energy eigenvalues $\{E_\alpha/n\}$ with $n = 16$	63
7.7	Diagonal matrix elements $\langle \alpha \sigma_z^1 \alpha \rangle$ of a single-qubit σ_z operator on vertex 1 of \mathcal{G} as a function of rescaled energy eigenvalues $\{E_\alpha/n\}$ with $n = 14$	64
7.8	Left: Diagonal matrix elements for the interaction term h^{67} of the integrable 1D hopping Hamiltonian where $n = 14$, Right: Diagonal variance $v_D(0)$ for $E = 0$ for $n = 10, 12, 14, 18$	64
7.9	Envelope function $f(\tilde{E}, \omega)$ evaluated at $\tilde{E} = 0$ for the empirical variance of off-diagonal matrix elements $\langle \alpha h^{12} \beta \rangle$ of the interaction term h^{12} between a pair of neighboring vertices on \mathcal{G} with $n = 14$	65
7.10	Envelope function $f(\tilde{E}, \omega)$ evaluated at $\tilde{E} = 0$ for the empirical variance of off-diagonal matrix elements $\langle \alpha \sigma_z^1 \beta \rangle$ single-qubit σ_z operator on site 1 with $n = 14$	65
7.11	Local purity \mathcal{P}_1 of the eigenstates of H as a function of energy eigenvalue with $n=14$	66

7.12	Bi-local \mathcal{P}_2 and 3-local \mathcal{P}_3 of the eigenstates of H as a function of energy eigenvalue with $n=14$	66
7.13	Top: Time evolution for an interaction term $\langle h(t) \rangle$ for a random 3-regular graph and an 1D open chain with $n = 14$. Bottom: Time evolution for $\langle \sigma_z(t) \rangle$	68

Chapter 1

Introduction: Motivations and Overview

An important way in which quantum mechanics departs from classical mechanics is the fact that a pure state can be described by a vector in a discrete Hilbert space of a potentially large dimension, compared to the number of coordinates, rather than by a point in a phase space. For a many-body system the dimension N of the state space grows exponentially as $N = 2^n$ with the number n of constituent parts. This fact allows for some advantages of quantum computing over classical computing models, but also makes exact calculations of many-body eigenstates and expectation values a hopelessly complicated task. In particular, since quantum states are represented by vectors, the notion of a random state of a quantum system is more subtle and involves more complexity than classical randomness. Since, as in classical dynamics, quantum evolution is a transformation on the state space, the fact that quantum states are Hilbert space vectors requires that random quantum dynamical processes be understood in terms of random *unitary* transformations.

In classical information processing, the use of randomized algorithms and techniques has been extensively explored. Recently, the quantum information community has asked the parallel question for quantum computation, namely, what quantum information processing tasks can be performed or improved if one has access to random quantum states and unitary transformations, and what does the

assumption of random states and unitary transformations permit one to prove that may be difficult or impossible otherwise. Several applications have been developed, perhaps most notably, that the strength of a noisy quantum channel can be estimated in an efficient and unbiased way by *twirling* the channel with a random unitary transformation [1]. Other examples include, fast "scrambling" of information, efficient quantum tomography and randomized gate benchmarking [2, 3, 4].

It has been shown that parallel to a result from classical computation theory, random unitary transformations are good encoders of quantum information. Specifically, a mapping from a logical Hilbert space of k -qubits to a random subsystem of an $n > k$ qubit system, has been shown to saturate the quantum erasure channel. This result has been applied to the problem of the black hole information paradox [5]. Strikingly, a pair of channels for which the minimum output entropy is not additive can be shown to occur with finite probability through a randomized construction [6].

Nevertheless, it can be shown that to generate an arbitrary unitary transformation on the state space of an n -qubit system requires a number of single and two-qubit gates that grows exponentially with n . But this need not be as severe a setback as it appears, since not all protocols which assume access to random unitary transformations require a fully random unitary transformation with respect to the Haar measure. It has been useful to classify protocols by the minimum required order moments that are required to be equivalent to the Haar measure. A distribution which requires only moments of up to order t is referred to as a unitary t -design [1]. Many algorithms, notably encoding and twirling protocols require only a 2-design, which has been shown to require only $\mathcal{O}(n \log n)$ gates [7].

Perhaps the simplest way to construct random unitary transformations is by selecting gates at random from a universal gate set. So-called random quantum circuits were first introduced in [11] and were suggested as a method for efficient twirling in [1]. The extent to which random quantum circuits are efficient t -designs was raised in [7] and proved to be efficient in n for the case $t = 1$ and $t = 2$. In the first part of this thesis I will examine the question of how quickly moments of arbitrary order t of random quantum circuits converge to the Haar measure, as well as how some aspects of random quantum circuit design influence the convergence rates.

In Chapter 1 mathematical tools will be presented for analyzing the convergence rate of random quantum circuits to the Haar measure. It will be shown that the convergence rate for t -order moments is determined by the properties of a superoperator describing the action of the random

quantum circuit on t -copies of the system. In Chapter 3 random quantum circuits which are reversible, for which corresponding moment superoperator is Hermitian, will be examined. Bounds will be constructed relating the gap between the largest and second largest eigenvalue of the moment superoperator corresponding to different design parameters for random quantum circuits. As reported in [19], it will be shown for a class of random quantum circuits which is invariant under permutations of the qubit labels, that for sufficiently large n , and for any t the gap and hence the convergence rate scales as $1/n$. The relationship between the gate complexity of typical unitary transformations and the linear asymptotic scaling result for the convergence time of finite order moments will be discussed. In Chapter 4, *irreversible* random quantum circuits, for which the moment superoperator is not Hermitian, will be discussed. It will be shown that the optimal convergence rate for second order moments of any permutationally invariant random quantum is achieved using an irreversible gate distribution suggested by an implementation of a random quantum circuit as a measurement pattern on a cluster state. [20].

In the remainder of this thesis, so-called many-body quantum chaos is examined. It was first suggested by Wigner [8] that the eigenvalues and eigenvectors of a complex quantum many-body Hamiltonian ought to have the same statistical features as certain ensembles of random matrices. It was later noticed that this property also holds for quantized versions of classically chaotic systems. That is, for strongly non-integrable quantum Hamiltonians the eigenvectors and eigenvalues appear random with respect to an appropriately defined measure on the Hilbert space. Similar to the occurrence of phase-space mixing and ergodicity in classical systems, the randomness of the eigenvectors of a chaotic quantum Hamiltonian suggests that the corresponding propagator acts as a random unitary transformation, and thus randomizes initial states. However, since the Hamiltonian is fixed and depends on only a small number of parameters compared to the dimension of the system Hilbert space, the resulting dynamics is not characterized by true randomness but is pseudo-random. I investigate the properties of chaotic many-body systems, such as interacting spin-1/2 (qubits) systems. I will generalize well known conjectures and results from semiclassical quantum chaos, which pertains to the large energy limit of quantum systems for which a classically chaotic limit exists, to the thermodynamic limit of quantum many-body systems. For such systems, the idea of chaos can not be borrowed from a corresponding classical notion, but must be constructed solely out of

inherently quantum aspects of the system's static and dynamical properties. The implications of quantum chaos research to the foundation for classical statistical mechanics is discussed.

Chapter 5 contains an introduction to quantum chaos in general, in particular it introduces standard conjectures and results relating smoothly varying statistical properties of the eigenvectors and eigenvalues to classical quantities. Some problems in relating classical concepts such as integrability to many-body quantum systems is discussed. In Chapter 6, a method of formulating weak constraints for the statistical properties of many body systems in the thermodynamic limit is presented. The method builds on techniques introduced in [9] and [10] which employs orthogonal polynomials with respect to the density of states of the system Hamiltonian to express smoothed properties of the eigenvectors in the thermodynamic limit. In Chapter 7, a numerical study of the spin-1/2 XX Hamiltonian on a 3-regular random graph is presented to illustrate and support the results of Chapter 6. Conclusions follow in Chapter 8 along with a discussion of future research directions.

Chapter 2

Random Quantum Circuits: Background

2.1 Convergence of Random Quantum Circuits

In this chapter the mathematical machinery for analyzing the convergence properties of random quantum circuits, is introduced. Let a k -length random quantum circuit acting on n qubits be a sequence of k randomly selected unitary transformations $U_k \dots U_1$, where each U_i is an element of the unitary group $U(N)$ for $N = 2^n$. Each U_i is selected independently according to a measure $\mu(W)$, defined on all subsets $W \subseteq U(N)$. If μ has support on a universal gate set, then it follows that the measure μ_k generated by k -length random quantum circuits, $U = U_k \dots U_1$, converges [12] as $k \rightarrow \infty$ to the unique measure on $U(N)$, referred to as the Haar measure and denoted μ_H which is invariant under the group action of arbitrary elements of $U(N)$ [13]. That is, $\mu_H(W) = \mu_H(W')$ for any two subsets A and W' of $U(N)$, such that W' is the image of W under some $U \in U(N)$. The central question addressed in the first part of this thesis is how large k must be for the distance $\|\mu_k - \mu_H\|$ to be small in an appropriate sense. The answer will in general depend on the norm chosen. Some standard norms and a family of norms motivated by applications to quantum information processing will also be discussed.

A natural distance between probability distributions is the so-called *total variation distance*, which is given by the largest difference in probability between $\mu_k(W)$ and $\mu_H(W)$ for any $W \subseteq U(N)$, that is,

$$\|\mu_k - \mu_H\|_{TV} = \sup_{W \subseteq U(N)} |\mu_k(W) - \mu_H(W)|.$$

Restricted to A consisting of the union of bounded regions of $U(N)$, the total variation is the L^1 norm on the probability densities

$$\|\mu_k - \mu_H\|_{TV} = \int_{U \in U(N)} |d\mu_k(U) - d\mu_H(U)|.$$

Uniform convergence of the probability densities, on the other hand, is stronger and requires closeness in the L^∞ norm, namely,

$$\|\mu_k - \mu_H\|_\infty = \sup_{U \in (U(N))} \left| \int_{U' \in U(N)} d\mu_k(U') \delta(U' - U) - \int_{U' \in U(N)} d\mu_H(U') \delta(U' - U) \right|.$$

Uniform convergence is too strong even for classical probability distributions, since the total variation distance limits the distinguishability of distributions over classical states. In quantum information processing application, a unitary transformation U describing the evolution of quantum states of some system S cannot be accessed directly, but only indirectly through measurements made on quantum states that are evolved by U . Specifically, in order to distinguish between two unitary transformations, U and U' , one needs to prepare an initial state ρ that acts on the tensor product space of the state spaces of the system S and an ancilla system A , evolve ρ under $U \otimes I_A$, $\rho' = U \otimes I_A \rho U^\dagger \otimes I_A$, and then perform a measurement on ρ' . Given the ability to prepare arbitrary initial states and perform arbitrary measurements on the output, it follows from Helstrom's theorem [14] that distinguishability of two unitary transformations U and U' is determined by

$$\sup_\rho \|(U \otimes I_A) \rho (U^\dagger \otimes I_A) - (U' \otimes I_A) \rho (U'^\dagger \otimes I_A)\|_1,$$

where $\|X\|_1 \equiv \text{tr}(\sqrt{X^\dagger X})$. Taking the supremum over all dimensions N_A of the ancilla space yields the diamond norm [15], the most general metric for distinguishability of quantum states. The

diamond can be extended to unitary transformations and completely positive maps, by taking the supremum over all states acted upon.

When distinguishing two distributions over the set of unitary transformations, an additional consideration is important. Suppose there is a source that produces a sequence of random unitary transformations selected independently according to μ . An experimenter may prepare any initial state of system plus ancilla, evolve the state with U and perform any measurement. A complete description of this process is provided by the quantum channel,

$$M_1[\mu](\rho) = \int_{U \in U(N)} d\mu(U) U \rho U^\dagger, \quad \forall \rho.$$

It is convenient to express M_1 in Liouville representation, that is, as a linear operator acting on the vector space of linear operators \mathcal{H}_{op} on \mathcal{H} of dimension N^2 . Borrowing notation from open-system theory [16], “operator kets” in \mathcal{H}_{op} are introduced denoted as $|A\rangle\rangle \equiv A$ and $\langle\langle A| = A^\dagger$. Accordingly, an N^2 -dimensional operator ket transforms according to $(U \otimes U^*)|A\rangle\rangle \equiv UAU^\dagger$, under $U \in U(N)$. Then,

$$M_1[\mu] = \int_{U \in U(N)} d\mu(U) U \otimes U^*.$$

Once a basis of \mathcal{H}_{op} is chosen, the matrix elements of $U \otimes U^*$ consists of a complete set of (1,1) monomials of the matrix elements of U , that is, monomials of the form $u_{ij}u_{kl}^*$. Thus, the components of M_1 are a complete set of (1,1) order moments of μ . Since M_1 only contains the first-order moments of μ , any two distributions μ and μ' which share the same first-order moments are not physically distinguishable.

If the source is modified so that at each sampling of μ , the source produces t *identical copies* of U , then additional information about μ can be obtained. This situation can be completely described by the quantum channel

$$M_t[\mu](\rho) = \int_{U \in U(N)} d\mu(U) U^{\otimes t} \rho \otimes U^{\dagger \otimes t},$$

whereby $\forall |\rho\rangle\rangle$

$$M_t[\mu] = \int_{U \in U(N)} d\mu(U) U^{\otimes t} \otimes U^{*\otimes t} \equiv \int_{U \in U(N)} d\mu(U) U^{\otimes t, t}. \quad (2.1)$$

Note that the object $U^{\otimes t, t}$ contains all of the (t, t) -order monomials of the matrix elements of U , (e.g. $u_{i_1 j_1} \dots u_{i_t j_t} u_{k_1 l_1}^* \dots u_{k_t l_t}^*$), and the matrix elements of M_t provide a complete set of t -order moments of $\mu(U)$. Thus, any two distributions μ and μ' that differ for some moment of order up to t can be distinguished. Equivalently, if a particular protocol involves selecting any finite number of copies t of the same randomly sampled unitary transformations, then any distribution which shares the same moments up to order t can be substituted without any observable difference. The notion of a distribution μ which has the same distribution as the Haar measure up to moments of order t was first introduced in [1], and is referred to as an exact unitary t -design. If the moments up to order t are approximately the same as the Haar measure, such that

$$\sup_{\rho} \|M_t[\mu_k] \otimes I_A[\rho] - M_t[\mu_H] \otimes I_A[\rho]\|_1 < \epsilon,$$

where the supremum is taken over density matrices ρ that act on $\mathcal{H}^{\otimes t} \otimes \mathcal{H}_A$, then μ is referred to as an ϵ -approximate unitary t -design [1].

2.2 Tools from Harmonic Analysis

The probability density $d\mu_k(U)$ of a k -length random quantum circuit where each gate is selected independently according to $d\mu(U)$, is given by the k -fold convolution,

$$d\mu_k(U) = \int \prod_{i=1}^k d\mu(U_i) \delta(U - \prod_{i=1}^k U_i)$$

of $d\mu(U)$. A powerful technique for examining how a distribution over a compact group behaves under convolution is provided by harmonic analysis [17]. By the Peter-Weyl theorem, the Hilbert space of square integrable functions on any compact group is spanned by the finite-dimensional irreducible representations (irreps) of the group. Next, define $\{D^s(U)\}$ as the set of such finite dimensional irreps of $U(N)$ and let d_s be the dimension of each representation. Then, different irreps are orthogonal with respect to the Haar measure on the group, in the sense that

$$\int_{U(N)} d\mu_H(U) [D_{ij}^s(U)]^* D_{kl}^{s'}(U) = \frac{1}{d_s} \delta_{ss'} \delta_{ik} \delta_{jl}.$$

So, any function $f(U)$ may be expanded as a series

$$f(U) = \sum_{s=0}^{\infty} \sum_{ij}^{d_s} f_{ij}^s D_{ij}^s(U),$$

where the Fourier coefficient

$$f_{ij}^s = d_s \int d\mu_H(U) f(U) [D_{ij}^s(U)]^*.$$

If, in addition, $f(U)$ is continuous, then the sequence of partial sums converges uniformly, that is, for any $\epsilon > 0$, there exists an s' such that

$$\left| f(U) - \sum_{s=0}^{s'} \sum_{ij} f_{ij}^s D_{ij}^s(U) \right| < \epsilon,$$

$\forall U \in U(N)$. Furthermore, the convolution of two functions, $f(U)$ and $g(U)$, is straightforward to compute in terms of the corresponding Fourier expansions. Let $(f \circ g)(U) = \int d\mu_H(U') f(U) g(U'^{\dagger}U)$, be the convolution of $f(U)$ and $g(U)$. Then,

$$\begin{aligned} (f \circ g)^s &= \int d\mu_H(U) (f \circ g)(U) [D^s]^*(U) \\ &= \int \int d\mu_H(U) d\mu_H(U') f(U) g(U'^{\dagger}U) [D^s]^*(U), \end{aligned} \quad (2.2)$$

Now let $U'^{\dagger}U \rightarrow U'$ and $UU'^{\dagger} \rightarrow U$. Then,

$$\begin{aligned} (f \circ g)^s &= \int \int d\mu_H(U) d\mu_H(U') f(U) g(U') [D^s]^*(UU') \\ &= \int \int d\mu_H(U) d\mu_H(U') f(U) g(U') [D^s]^*(U) [D^s]^*(U') \\ &= \int d\mu_H(U) f(U) [D^s]^*(U) \int d\mu_H(U') g(U') [D^s]^*(U') \\ &= f^s g^s. \end{aligned} \quad (2.3)$$

Thus, under convolution, the matrix of Fourier coefficients corresponding to each irrep $(f \circ g)^s$ is given by the matrix product of the coefficient matrices f^s and g^s corresponding to the same irrep

of the functions to be convolved.

If μ is absolutely continuous, then its density $d\mu(U) = p(U)d\mu_H(U)$ exists, and the convergence of μ_k can be understood in terms of the Fourier components $\{p^s\}$. Otherwise, the convergence of the set of expectation values of all square integrable functions $\mathbb{E}[f(U)]$ can be used to define the convergence of μ_k .

2.3 Convergence of Moments

Since $U^{\otimes t,t}$ is also a representation of $U(N)$, the convolution of the t -order moments is given by the matrix product,

$$\begin{aligned} M_t[\mu_k] &= \int \prod_{i=1}^k d\mu(U_i) \prod_{i=1}^k U_i^{\otimes t,t} \\ &= \prod_{i=1}^k \int d\mu(U_i) U_i^{t,t} \\ &= (M_t[\mu])^k. \end{aligned} \tag{2.4}$$

If the measure μ is invariant under Hermitian conjugation, that is $\mu(A) = \mu(A')$ where $U \in A \iff U^\dagger \in A'$ for every $A \subseteq U(N)$, then the moment superoperator obeys the property

$$M_t[\mu] = \int d\mu(U) U^{\otimes t,t} = \int d\mu(U) U^{\dagger \otimes t,t} = M_t[\mu]^\dagger.$$

A random quantum circuit selected according to any such distribution will be referred to as *reversible*. I will present here the argument shown in [19], that the moments of μ_k converge to those of the Haar measure μ_H as $k \rightarrow \infty$ for any reversible random quantum circuit as long as μ has support on a universal subset of $U(N)$. Let \mathcal{V}_t be the subspace of fixed points of $U^{\otimes t,t}$, $U \in U(N)$, with $\mathcal{P}_{\mathcal{V}_t}$ denoting the corresponding projector. It will be shown that

$$\lim_{k \rightarrow \infty} (M_t[\mu])^k = \mathcal{P}_{\mathcal{V}_t} = M_t[\mu_H], \tag{2.5}$$

where $P_{\mathcal{V}}$ is the projector onto \mathcal{V} . Let $|\phi\rangle\rangle$ be an eigenvector of $M_t[\mu]$, and $|\phi_U\rangle\rangle \equiv U^{\otimes t,t}|\phi\rangle\rangle$. From the triangle inequality it follows that

$$|\langle\langle\phi|M_t[\mu]|\phi\rangle\rangle| = \left| \int d\mu(U) \langle\langle\phi|U^{\otimes t,t}|\phi\rangle\rangle \right| \leq \int d\mu(U) |\langle\langle\phi|\phi_U\rangle\rangle|.$$

Thus, $\lambda \leq 1$ with equality holding if and only if $U^{\otimes t,t}|\phi\rangle\rangle = |\phi\rangle\rangle, \forall U \in U(N)$. Furthermore, if the support of μ is universal, for any open ball in $U(N)$ there is a U , such that $U = U_k \dots U_1$ where each U_i is in the support of μ . Therefore, if $|\phi\rangle\rangle \in \mathcal{V}_t$ then $U|\phi\rangle\rangle = |\phi\rangle\rangle$ for all $U \in U(N)$.

Since all other eigenvalues of $M_t[\mu]$ have magnitude less than 1, $M_t^k[\mu]$ converges to $\mathcal{P}_{\mathcal{V}_t}$. To establish the second equality in Eq. (2.5), we invoke the invariance of the Haar measure under $U(N)$, $\mu_H(U) = \mu_H(U'U)$. For $|\phi\rangle\rangle$, an eigenoperator of $M_t[\mu_H]$ with eigenvalue λ , it follows that $M_t[\mu_H]|\phi\rangle\rangle = \int d\mu_H(U) U^{\otimes t,t}|\phi\rangle\rangle = \lambda|\phi\rangle\rangle$. Thus,

$$\begin{aligned} U'^{\otimes t,t} \lambda |\phi\rangle\rangle &= \int d\mu_H(U) (U'U)^{\otimes t,t} |\phi\rangle\rangle \\ &= \int d\mu_H(U'^t U) U^{\otimes t,t} |\phi\rangle\rangle \\ &= \int d\mu_H(U) U^{\otimes t,t} |\phi\rangle\rangle \\ &= \lambda |\phi\rangle\rangle. \end{aligned}$$

If $\lambda \neq 0$, it follows that $|\phi\rangle\rangle \in \mathcal{V}_t$, otherwise $\lambda = 0$, which establishes the desired result. The above result also holds with λ replaced by $|\lambda|$ for irreversible circuits that are diagonalizable, since only the absence of Jordan blocks of dimension more than one was assumed. A general proof of Eq. (2.5) is contained in Lemma 3.2 in [7].

2.3.1 Convergence Rate and Convergence Time

Having shown that the moment superoperator $M_t^k[\mu]$ converges to $M_t[\mu_H]$, for reversible random quantum circuits, one may determine the *rate* at which convergence occurs in terms of circuit depth k . Since $M_t[\mu_H]$ projects onto the eigenspace of $M_t[\mu]$ of eigenvalue 1, the distance $\|M_t^k[\mu] - M_t[\mu_H]\|$ with respect to any norm depends only on the remaining eigenvalues $\{\lambda_i\}$ of $M_t[\mu]$ and the corresponding eigenprojectors $\{\Pi_i\}$. Specifically, if k is sufficiently large, $\|M_t^k[\mu] - M_t[\mu_H]\| =$

$\left\| \sum_{\lambda_i \neq 1} \lambda_i^k \Pi_i \right\| \approx |\lambda_1|^k \|\Pi_1\|$, where $\lambda_1 \equiv 1 - \Delta_t$ is the subdominant eigenvalue of $M_t[\mu]$. Thus, the asymptotic convergence rate, $\Gamma = -\ln(1 - \Delta)$, is entirely determined by the spectral gap Δ_t of $M_t[\mu]$.

In order to determine the convergence time, an upper-bound of the circuit length is required to achieve a specified accuracy, ϵ . Let the convergence time, with respect to a given norm, be defined by the minimum length k_c for which $\|M_t^{k_c}[\mu] - M_t[\mu_H]\| \leq \epsilon$. For the case where there is no ancilla, the diamond norm becomes the 1-norm on the space of $t * n$ qubit density matrices. One may bound the 1-norm starting from the 2-norm [7]. For any density matrix ρ , $\|(M_t^k[\mu] - M_t[\mu_H])(\rho)\|_2 \leq \lambda_1^k$. This follows from normalization of ρ and the fact that $M_t[\mu_H]$ projects onto the eigenspace of eigenvalue 1 of $M_t[\mu]$. In conjunction with the Cauchy-Schwartz inequality, this implies $\|(M_t^k[\mu] - M_t[\mu_H])(\rho)\|_1 \leq 2^{nt} \lambda_1^k$. Requiring that $2^{nt} \lambda_1^{k_c} \leq \epsilon$ finally yields

$$k_c \leq \Delta_t^{-1}(\log(1/\epsilon) + nt \log(2)). \quad (2.6)$$

Chapter 3

Reversible Random Quantum Circuits

If the measure μ is invariant under Hermitian conjugation, as noted in Chapter 2, then the moment superoperator is Hermitian, and the corresponding random quantum circuit is *reversible*. In this chapter, I will review the main results in [19]. Specifically, I will analyze a class of reversible random quantum circuits with the following form: at each time step, a gate will be selected independently from a distribution $\tilde{\mu}$ which has support on a universal subset of $U(4)$ and is invariant under Hermitian conjugation.

The gate is subsequently applied to a pair (i, j) of qubits selected according to a probability distribution p_{ij} . Since each gate in the random quantum circuit only acts on a fixed pair of qubits, it is convenient to construct an alternative tensor product decomposition of the state space, \mathcal{H}_{M_t} upon which the moment operator M_t acts. Recall that $\mathcal{H}_{M_t} = \mathcal{H}^{\otimes 2t}$ where $\mathcal{H} = \mathcal{H}_q^{\otimes n}$ is the Hilbert space upon which the random quantum circuit acts and consists of the tensor product space of n two-dimensional Hilbert spaces \mathcal{H}_q . One may instead define a local moment space, $\mathcal{H}_{l_t} = \mathcal{H}_q^{\otimes 2t}$, consisting of the $2t$ factor spaces associated with a single qubit on each of the $2t$ copies of \mathcal{H} , and now write $\mathcal{H}_{M_t} = \mathcal{H}_{l_t}^{\otimes n}$ as in Fig. 3.1. Since for each application of a random gate U to a fixed pair of qubits, $U^{\otimes t, t}$ acts non-trivially only on the associated bi-local moment space $\mathcal{H}_{l_t} \otimes \mathcal{H}_{l_t}$, the

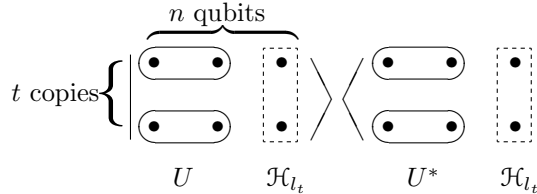


Figure 3.1: It is convenient to visualize the moment space \mathcal{H}_{M_t} as an array of $2n$ qubits, with each tn qubits forming a bra and tn qubits forming a ket. The two columns, one in the bra and the other in the ket, which correspond to a single qubit determine the local moment spaces \mathcal{H}_{l_t} . The action of a two-qubit gate U is shown only to affect bi-local moment spaces $\mathcal{H}_{l_t} \otimes \mathcal{H}_{l_t}$ corresponding to the relevant qubit pair.

moment operator may be written as

$$M_t[\mu] = \sum_{i < j}^n p_{ij} m_t^{ij}[\tilde{\mu}], \quad (3.1)$$

where the restriction of m_t^{ij} to the corresponding bi-local moment space $\mathcal{H}_{l_t} \otimes \mathcal{H}_{l_t}$ is

$$m_t[\tilde{\mu}] = \int_{U \in U(4)} d\tilde{\mu}(U) U^{\otimes t, t}.$$

Thus, for any reversible random quantum circuit consisting of independently chosen single- and two-qubit gates, the corresponding t -order moment operator has the form of a many-body Hamiltonian. The rate at which the moments of order t converge to their Haar measure is given by the gap $\Delta = 1 - \lambda_1$ between the largest eigenvalue of 1 and the subdominant eigenvalue λ_1 .

3.1 Extremal State Subspace

Several properties of the extremal eigenspace \mathcal{V}_t of the fixed points of $M_t[\mu]$ will be demonstrated. Recall from Eq.(2.5) that \mathcal{V}_t consists of operators in \mathcal{H}_{M_t} that commute with all t -fold tensor power unitaries $U^{\otimes t}$. By Schur-Weyl duality [7, 21], every such operator is a linear combination of elements of the symmetric group, \mathcal{S}_t , of permutations of the t -copies of \mathcal{H} in $\mathcal{H}^{\otimes t}$. One may write any such permutation as

$$|\sigma^{(n)}\rangle\rangle = \sum_{i_1 \dots i_t = 1}^N |i_1 \dots i_t\rangle \langle i_{\sigma(1)} \dots i_{\sigma(t)}|,$$

where $\sigma \in \mathcal{S}_t$. Furthermore, each such permutation may be viewed as a *product state* relative to the factorization $\mathcal{H}_{M_t} = \mathcal{H}_{l_t}^{\otimes n}$. Explicitly, $|\sigma^{(n)}\rangle = (|\sigma\rangle)^{\otimes n}$, where

$$|\sigma\rangle = \sum_{i_1 \dots i_t = 0,1} |i_1 \dots i_t\rangle \langle i_{\sigma(1)} \dots i_{\sigma(t)}| \in \mathcal{H}_{l_t}.$$

The extremal eigenspace, \mathcal{V}_t , is thus exactly spanned by product states. One consequence of this highly atypical property is that M_t is *frustration free* [22], that is, if $|\phi\rangle$ maximizes the expectation value of M_t , then it also maximizes the expectation value of every term m_t^{ij} . Physically, factorization of the ground eigenspace can occur in certain spin systems in the presence of a *factorizing field* [23]. An extensive survey of spin-1/2 Hamiltonians in factorizing fields is performed in [24, 25]. The relationship between the gap of a many-body system and the extent of entanglement of the ground state is an area of active research [26, 27].

The extremal eigenspace \mathcal{V}_t in addition to being factorizable, is also identical for all $M_t[\mu]$ with universal μ . Consequently, inequalities can be derived between the gaps of $M_t[\mu]$ for different gate distributions, μ . Consider the moment operators, $M_t[\mu_1]$ and $M_t[\mu_2]$, for two gate distributions, μ_1 and μ_2 , that both have support on universal subsets of $U(N)$. Now let $\mu = p\mu_1 + (1-p)\mu_2$ where $0 \leq p \leq 1$. From the triangle inequality it follows that

$$\|M_t[\mu] - M_t[\mu_H]\|_{sp} \leq p\|M_t[\mu_1] - M_t[\mu_H]\|_{sp} + (1-p)\|M_t[\mu_2] - M_t[\mu_H]\|_{sp},$$

where $\|\cdot\|_{sp}$ is the spectral norm, that is since $\|M_t[\mu] - M_t[\mu_H]\|_{sp} = \lambda_1$ and $\Delta = 1 - \lambda_1$ it follows that,

$$\Delta \geq p\Delta_1 + (1-p)\Delta_2. \quad (3.2)$$

Thus, the gap of the moment superoperator of a random quantum circuit which can be expressed as a weighted average of simpler, though still universal, random quantum circuits is lower bounded by the average of the gaps corresponding to the constituent random quantum circuits.

As an application of Eq. (3.2), consider a random quantum circuit with coupling probabilities p_{ij} that satisfy only the requirement that there is a connected path from each i to each j such that p_{ij} is nonzero for every step. Let $\theta \in S_n$ be a permutation of the n qubit labels. I claim that $\theta M_t \theta^\dagger$ has

the same eigenvalues as M_t . To see this, now consider the convex sum $M_t = (n!)^{-1} \sum_{\theta \in S_n} \theta M_t \theta^\dagger$. Because the sum is invariant under permutations, it follows that $M_t = \frac{2}{n(n-1)} \sum_{i < j} m_t^{ij}$. From Eq. (3.2) it now follows that for any $\tilde{\mu}$ on $U(4)$, the distribution p_{ij} with the largest gap is given by the uniform distribution $p_{ij} = \frac{2}{n(n-1)} \forall i, j$.

Now let α be any nonintersecting 1D loop connecting all n -qubits. Let \mathcal{C} be a set of coupling probabilities, p_{ij} such that $p_{ij} = \sum_{\alpha} q_{\alpha} p_{ij}^{\alpha}$ where $\sum_{\alpha} q_{\alpha} = 1$ and $q_{\alpha} \geq 0$ and $p_{ij}^{\alpha} = 1/n$ for all nearest neighbors on α . The gap, Δ_1 , for each random quantum circuit with coupling probabilities p_{ij}^{α} , is the same, thus by Eq. (3.2) the gap, $\Delta_{\mathcal{C}}$, for the random quantum circuit corresponding to the set of coupling probabilities, \mathcal{C} , is at least as large as Δ_1 . This class includes not only the completely symmetric graph, but also any graph of nearest neighbors on the surface of a $(d+1)$ -dimensional sphere. Let the gap for the corresponding random quantum circuit be labeled Δ_d . It follows from Eq. (3.2) that $\Delta_{\infty} \geq \Delta_d \geq \Delta_1$, where Δ_{∞} is the gap of the permutation invariant random quantum circuit. Thus the gap of the 1D closed chain lower bounds the gap of all d -dimensional uniform random quantum circuits. Furthermore, the gap of a 1D open chain lower bounds the gap of the closed 1D chain, since one may average over all translations of open 1D chains to construct the closed chain.

In the previous example, the gate distribution $\tilde{\mu}$ on $U(4)$ is held fixed, while the distribution p_{ij} is varied. It is also possible to construct inequalities between the gaps when p_{ij} is fixed but $\tilde{\mu}$ is permitted to vary. Let $|\phi\rangle \in \mathcal{H}_M$. Let $\rho^{ij} = \text{tr}_{l \neq i, j}(|\phi\rangle\langle\phi|)$. It follows that $\langle\langle\phi|M_t|\phi\rangle\rangle = \sum_{i < j} p_{ij} \text{tr}(\rho^{ij} m_t)$. If one lets $\tilde{\rho} = \sum_{i < j} p_{ij} \rho^{ij}$, then $\langle\langle\phi|M_t|\phi\rangle\rangle = \text{tr}(\tilde{\rho} m_t)$. If $\tilde{\mu}$ is the Haar measure on $U(4)$, then m_t is the projector onto the invariant eigenspace \mathcal{V}_2 . Given a set of coupling probabilities, $\{p^{ij}\}$, there exists an operator ket $|A_1\rangle$ such that the projection into \mathcal{V}_2 of $\tilde{\rho}$ is a maximum. This must be satisfied by the first excited state of M_t . Let the eigenvalues of $m_t[\tilde{\mu}]$ be $\{e_i\}$. For $\tilde{\mu}_H$, $e_0 = 1$ and $e_i = 0 \forall i > 0$. For $\tilde{\mu} \neq \tilde{\mu}_H$, the eigenspace $|0\rangle$ is \mathcal{V}_2 the same as for $\mu_H(U)$, since it is the same for every universal gate distribution, but the remaining eigenvalues are no longer non-zero, but must satisfy $1 < e_i < -1$ because μ is universal. Let $\tilde{\rho} = \sum_i p_i |i\rangle\langle i|$. Then $\text{tr}(\tilde{\rho} m_t) = \sum_i e_i p_i$. The largest possible value of this sum for $\langle\langle A|\sigma\rangle\rangle \forall \sigma$ is given by $p_0 e_0 + (1 - p_0) e_1$, where e_{min} is the smallest eigenvalue of m_t . This yields bounds on the gap of M_t of $\Delta_H(1 - e_1) \leq \Delta_{\mu} \leq \Delta_H(1 - e_{min})$. Since the eigenvalues of m_t do not depend on n , although they depend on t , for any set of coupling

probabilities, the gate distribution $\tilde{\mu}$ on $U(4)$ does not affect the scaling of the gap with n .

Furthermore, since the eigenvalues of $M_t = \sum_{i<j} p_{ij} m_t^{ij}$ are invariant under local unitary transformations (say what this means), it follows that the largest gap for any reversible gate set is obtained by averaging over all local unitary transformations, that is, given any $\tilde{\mu}$ the distribution obtained by averaging over local unitaries has a gap at least as large.

3.2 Permutationally Invariant Random Quantum Circuits

This section follows closely the arguments presented in [19]. If pairs of qubits are selected uniformly at random, the corresponding many-body Hamiltonian is invariant under permutations on the qubit labels, and the gap can be determined using a well-established (but not rigorously proven) mean-field technique, which for sufficiently large n yields an exact value for the gap. Such circuits will be generally referred to as *permutationally invariant random quantum circuits*. The corresponding moment operator may be written as follows:

$$M_t[\mu] = \frac{2}{n(n-1)} \sum_{i<j=1}^n m_t^{ij}[\tilde{\mu}]. \quad (3.3)$$

Since $M_t[\mu]$ is invariant under the symmetric group \mathcal{S}_n of permutations of the n local moment spaces, one may represent $M_t[\mu]$ in terms of completely symmetric generators of $U(d)$. Explicitly, if $\{b_{\alpha\beta}^i = |\alpha\rangle\rangle\langle\langle\beta|\}$ denotes an outer-product basis for operators acting on any \mathcal{H}_t , we may expand

$$m_t^{ij} = \sum_{\alpha\beta\gamma\delta=1}^d \langle\langle\alpha\gamma|m_t|\beta\delta\rangle\rangle b_{\alpha\beta}^i b_{\gamma\delta}^j \equiv \sum_{\alpha\beta\gamma\delta=1}^d c_{\alpha\beta\gamma\delta} b_{\alpha\beta}^i b_{\gamma\delta}^j,$$

and rewrite $M_t[\mu]$ as a quadratic function of the collective operators $B_{\alpha\beta} = \sum_{i=1}^n b_{\alpha\beta}^i$, that is,

$$M_t[\mu] = \frac{1}{n(n-1)} \sum_{\alpha\beta\gamma\delta=1}^d c_{\alpha\beta\gamma\delta} (B_{\alpha\beta} B_{\gamma\delta} - \delta_{\beta\gamma} B_{\alpha\delta}).$$

Since the operators $B_{\alpha\beta}$ obey $U(d)$ commutation rules, namely,

$$[B_{\alpha\beta}, B_{\gamma\delta}] = B_{\alpha\delta} \delta_{\beta\gamma} - B_{\beta\gamma} \delta_{\alpha\delta},$$

\mathcal{H}_{M_t} carries the (reducible) collective n -fold tensor product representation of $U(d)$. Thanks to the invariance under \mathcal{S}_n , each of the eigenoperators of $M_t[\mu]$ belongs to an irrep of $SU(d)$.

For the completely symmetric irrep, one may realize the $U(d)$ algebra in terms of d canonical Schwinger boson operators $\{a_\alpha, a_\alpha^\dagger\}$ [28]. That is, we let $B_{\alpha\beta} = a_\alpha^\dagger a_\beta$ and rewrite

$$M_t[\mu] = \frac{1}{n(n-1)} \sum_{\alpha\beta\gamma\delta=1}^d c_{\alpha\beta\gamma\delta} a_\alpha^\dagger a_\gamma^\dagger a_\beta a_\delta. \quad (3.4)$$

Since the totally symmetric irrep of \mathcal{H}_{M_t} contains exactly n Schwinger bosons, it is possible to eliminate one boson mode by regarding it as “frozen” in the vacuum for a generalized Holstein-Primakoff transformation [28]. Specifically, let the local basis be chosen so that the frozen mode corresponds to $|\sigma\rangle$, and let

$$\theta(n) \equiv (n - \sum_{\alpha \neq \sigma} a_\alpha^\dagger a_\alpha)^{1/2},$$

with $a_\sigma^\dagger \rightarrow \theta(n)$, $a_\sigma \rightarrow \theta(n)$. Now expanding the square root in a Taylor series yields:

$$M_t[\mu] = 1 - \frac{1}{n} \sum_{\alpha\beta=1}^d E_{\alpha\beta} a_\alpha^\dagger a_\beta + \mathcal{O}(1/n^2), \quad (3.5)$$

where

$$E_{\alpha\beta} = 2(\delta_{\alpha\beta} - \langle\langle \sigma\alpha | m_t | \sigma\beta \rangle\rangle - \langle\langle \sigma\alpha | m_t | \beta\sigma \rangle\rangle). \quad (3.6)$$

Note that, there are no terms containing a_σ^\dagger , $a_\sigma^\dagger a_\alpha$ etc. that couple any boson mode α with the state $|\sigma\rangle^{\otimes n}$ since it is an exact eigenstate of M_t .

Thus, for any reversible permutationally invariant random quantum circuit, and for any fixed $t > 0$, the spectral gap may be expanded as

$$\Delta_t = \sum_{p=1}^{\infty} a_p(t) n^{-p} + \mathcal{O}(e^{-c(t)n}) = \frac{a_1(t)}{n} + \mathcal{O}\left(\frac{a_2(t)}{n^2}\right) + \mathcal{O}(e^{-c(t)n}). \quad (3.7)$$

where the exponential term arises from tunneling between degenerate “wells” associated with each product ground state, $|\sigma\rangle^{\otimes n}$.

3.2.1 Leading order coefficient

I will now show that $a_1 > 0$ as long as $\tilde{\mu}(U)$ is universal. This is equivalent to showing that $\langle\langle\sigma\alpha|m_t|\sigma\alpha\rangle\rangle + \langle\langle\sigma\alpha|m_t|\alpha\sigma\rangle\rangle < 1$, for any operator $|\alpha\rangle\rangle$ such that $\langle\langle\alpha|\sigma\rangle\rangle = 0$. Let

$$|\psi\rangle\rangle = \frac{1}{\sqrt{2}}(|\sigma\alpha\rangle\rangle + |\alpha\sigma\rangle\rangle).$$

Upon taking the expectation value with respect to m_t , we have

$$\langle\langle\psi|m_t|\psi\rangle\rangle = \frac{1}{2} \left(\langle\langle\sigma\alpha|m_t|\sigma\alpha\rangle\rangle + \langle\langle\sigma\alpha|m_t|\alpha\sigma\rangle\rangle + \langle\langle\alpha\sigma|m_t|\sigma\alpha\rangle\rangle + \langle\langle\alpha\sigma|m_t|\alpha\sigma\rangle\rangle \right).$$

Since M_t (and hence m_t) is invariant under interchange of any two qubits, $\langle\langle\alpha\sigma|m_t|\sigma\alpha\rangle\rangle = \langle\langle\sigma\alpha|m_t|\alpha\sigma\rangle\rangle$ and $\langle\langle\alpha\sigma|m_t|\alpha\sigma\rangle\rangle = \langle\langle\sigma\alpha|m_t|\sigma\alpha\rangle\rangle$, yielding

$$\langle\langle\psi|m_t|\psi\rangle\rangle = \langle\langle\sigma\alpha|m_t|\sigma\alpha\rangle\rangle + \langle\langle\sigma\alpha|m_t|\alpha\sigma\rangle\rangle.$$

Following from the properties of the invariant subspace \mathcal{V}_t established previously, $\langle\langle\psi|m_t|\psi\rangle\rangle = 1$ if and only if the operator $|\psi\rangle\rangle$ is invariant under arbitrary unitary transformations of the form $U^{\otimes t}$ with $U \in U(4)$, given that the corresponding two-qubit gate distribution $\tilde{\mu}(U)$ is universal on $U(4)$. Thus, we must show that there exists a unitary transformation $U \in U(4)$ such that

$$U^{\otimes t}(\sigma \otimes \alpha + \alpha \otimes \sigma)U^{\dagger \otimes t} \neq \sigma \otimes \alpha + \alpha \otimes \sigma.$$

(Recall that $|\alpha\rangle\rangle \equiv \alpha$). In fact, we may take the permutation $|\sigma\rangle\rangle$ to be the identity $|I\rangle\rangle$ without loss of generality. This follows upon noting that

$$\langle\langle\psi|m_t|\psi\rangle\rangle = \int d\tilde{\mu}(U) \text{tr}[\psi^\dagger U^{\otimes t} \psi U^{\dagger \otimes t}].$$

Since $\sigma U^{\otimes t} = U^{\otimes t} \sigma$ for all $U \in U(4)$, $\psi^\dagger \sigma U^{\otimes t} \sigma^\dagger \psi U^{\dagger \otimes t} = \psi^\dagger U^{\otimes t} \psi U^{\dagger \otimes t}$. Thus, $\sigma \otimes \alpha + \alpha \otimes \sigma$ has the same expectation value as $I \otimes \tilde{\alpha} + \tilde{\alpha} \otimes I$, where $\tilde{\alpha} = \sigma^\dagger \alpha$.

Any operator $|\tilde{\alpha}\rangle\rangle$ orthogonal to the identity may be expanded $\tilde{\alpha} = \sum_\nu c_\nu \sigma_{\nu_1}^1 \dots \sigma_{\nu_t}^t$, where

$\nu = (\nu_1, \dots, \nu_t)$, and $\nu_i \in \{0, 1, 2, 3\}$, with $\sigma_0 = I$, $\sigma_1 = \sigma_x$, $\sigma_2 = \sigma_y$, $\sigma_3 = \sigma_z$, and the sum ranges over all possible strings ν except the one where $\nu_i = 0 \forall i$. Thus, $\tilde{\alpha} \otimes I = \sum_{\nu} c_{\nu} \sigma_{\nu_1}^1 \otimes I^1 \dots \sigma_{\nu_t}^t \otimes I^t$. Now, under $U = \exp(\frac{\pi}{4} i \sigma_3 \otimes \sigma_3)$, the following transformations hold for Pauli operators:

$$\begin{aligned} \sigma_1 \otimes I &\mapsto -\sigma_2 \otimes \sigma_3, \\ \sigma_2 \otimes I &\mapsto \sigma_1 \otimes \sigma_3, \\ \sigma_3 \otimes I &\mapsto \sigma_3 \otimes I, \\ I \otimes \sigma_1 &\mapsto -\sigma_3 \otimes \sigma_2, \\ I \otimes \sigma_2 &\mapsto \sigma_3 \otimes \sigma_1, \\ I \otimes \sigma_3 &\mapsto I \otimes \sigma_3. \end{aligned}$$

Thus, for any $|\tilde{\alpha}\rangle\rangle$ with support on a Pauli string such that $\nu_i = 1$ or 2 for some i , there are terms in the expansion of $U^{\otimes t}(I \otimes \tilde{\alpha} + \tilde{\alpha} \otimes I)U^{\dagger \otimes t}$ which contain factors of the form $\sigma_2 \otimes \sigma_3$, $\sigma_3 \otimes \sigma_2$, $\sigma_1 \otimes \sigma_3$, and $\sigma_3 \otimes \sigma_1$. Since there are no such term in the expansion of $I \otimes \tilde{\alpha} + \tilde{\alpha} \otimes I$, it follows that $I \otimes \tilde{\alpha} + \tilde{\alpha} \otimes I$ is *not* invariant under $(\exp(\frac{\pi}{4} i \sigma_3 \otimes \sigma_3))^{\otimes t}$. Similarly, if $|\tilde{\alpha}\rangle\rangle$ has support on any Pauli string such that $\nu_i = 3$ or 2 for some i , then $I \otimes \tilde{\alpha} + \tilde{\alpha} \otimes I$ is not invariant under $(\exp(\frac{\pi}{4} i \sigma_1 \otimes \sigma_1))^{\otimes t}$. Since $|\tilde{\alpha}\rangle\rangle$ must belong to one of these two cases, the proof is complete. \blacksquare

3.2.2 Additional invariant subspaces

The diagonalization procedure described in Sec. 3.2 determines both the extremal and neighboring eigenvalues of M_t belonging to the totally symmetric irrep of $SU(d)$. Although expressed in terms of bosonic operators, the procedure is equivalent to a variational Ansatz whereby the trial wavefunction of the extremal state is of the form

$$|\phi\rangle\rangle^{\otimes n} = |\phi \dots \phi\rangle\rangle,$$

and the first excited state, corresponding to a single bosonic excitation, is of the form

$$|n_{\phi} = n - 1, n_{\alpha}=1\rangle\rangle \equiv \frac{1}{\sqrt{n}}(|\phi \dots \phi \alpha\rangle\rangle + \dots + |\alpha \phi \dots \phi\rangle\rangle).$$

In principle, it is possible that the subdominant eigenvalue may lie instead in the $SU(d)$ irrep which carries exactly one anti-symmetric pair of indexes. This can be accommodated by using a different variational Ansatz for the excited state to be minimized. If we choose a local basis in \mathcal{H}_{ℓ_t} that includes the fixed extremal permutation $|\sigma\rangle\rangle$, with the remaining local basis operators $|\alpha\rangle\rangle \neq |\sigma\rangle\rangle$ treated as excitation modes, the relevant single-excitation band is spanned by kets of the following form:

$$|n_\sigma = n - 1, n_\alpha=1\rangle\rangle \equiv \frac{1}{\sqrt{2}}(|\sigma \dots \sigma\rangle\rangle|\sigma\alpha\rangle\rangle - |\alpha\sigma\rangle\rangle),$$

with nonzero matrix elements:

$$\begin{aligned} \langle\langle n_\alpha = 1 | M_t | n_\beta = 1 \rangle\rangle &= \delta_{\alpha\beta} - \tilde{E}_{\alpha\beta}/n + \mathcal{O}(1/n^2), \\ \tilde{E}_{\alpha\beta} &= 2(1 - \langle\langle \sigma\alpha | m_t | \sigma\beta \rangle\rangle). \end{aligned}$$

Note that unlike in Eq. (3.6) the “exchange term” $\langle\langle \sigma\alpha | m_t | \beta\sigma \rangle\rangle$ is no longer present. Upon diagonalization of $\tilde{E}_{\alpha\beta}$, the subdominant eigenvalue a_1 is determined, with an identical $1/n$ scaling as found for the symmetric irrep. The possibility that the subdominant eigenvalue lies in this irrep may be removed *a priori* by imposing a natural additional restriction on the random quantum circuit, namely by requiring that the two-qubit gate distribution be invariant under the transformation S that swaps the two-qubits, that is, $\tilde{\mu}(SU) = \tilde{\mu}(US) = \tilde{\mu}(U)$.

3.3 Locally Invariant Random Quantum Circuits

As reported in [19], a stronger result for the asymptotic convergence rate may be obtained for a subclass of permutationally invariant random quantum circuits which are, in addition, *locally invariant*, that is, $\tilde{\mu}(U)$ is invariant under the subgroup $U(2) \times U(2) \subset U(4)$ of local unitary transformations on the two target qubits. Specifically, I will now show that for locally invariant random quantum circuits the leading order coefficient a_1 of the $1/n$ expansion does not depend on t .

Recall that a_1 is determined by the maximum value of $\langle\langle \sigma\omega | m_t | \sigma\omega \rangle\rangle + \langle\langle \sigma\omega | m_t | \omega\sigma \rangle\rangle$, where $\sigma \in \mathcal{S}_t$ and $|\omega\rangle\rangle$ is a $U(2)$ invariant which is orthogonal to $|\sigma\rangle\rangle$. As shown previously, we may take $|\sigma\rangle\rangle$ to be the identity without loss of generality. Now, any operator orthogonal to the identity may

be expanded as $\omega = \sum_{\nu} c_{\nu} \sigma_{\nu_1}^1 \dots \sigma_{\nu_t}^t$ where, as before, $\nu = (\nu_1, \dots, \nu_t)$, and $\nu_i \in \{0, 1, 2, 3\}$, with $\sigma_0 = I$, $\sigma_1 = \sigma_x$, $\sigma_2 = \sigma_y$, $\sigma_3 = \sigma_z$, and the sum ranges over all possible strings ν except the one where $\nu_i = 0 \forall i$.

The first step is to show that the expectation value $\langle\langle I\omega|U^{\otimes t,t}|I\omega\rangle\rangle$ for any $U \in U(4)$ may be written as a symmetric polynomial of the form

$$\langle\langle I\omega|U^{\otimes t,t}|I\omega\rangle\rangle = \sum_{2 \leq p_1 + p_2 + p_3 \leq t} w_{\vec{p}} x^{p_1} y^{p_2} z^{p_3}, \quad (3.8)$$

where x, y, z are real numbers in $[-1, 1]$ which depend only on U , and $w_{\vec{p}}$ are positive coefficients which depend only on $|\omega\rangle\rangle$, with $\vec{p} = (p_1, p_2, p_3)$ and p_i being non-negative integers subject to $2 \leq p_1 + p_2 + p_3 \leq t$.

To establish Eq. (3.8) above, we exploit the fact that an arbitrary element of $U(4)$ may be written in the canonical decomposition form $U = U_1 \otimes U_2 U(q, r, s) U'_1 \otimes U'_2$, where U_1, U'_1, U_2, U'_2 act locally on either of two qubits and $U(q, r, s) = \exp\{i(q\sigma_1 \otimes \sigma_1 + r\sigma_2 \otimes \sigma_2 + s\sigma_3 \otimes \sigma_3)\}$ [29]. Since $|\omega\rangle\rangle$ is a $U(2)$ invariant, it then suffices to consider the action of $U(q, r, s)$. Direct calculation shows that under $U(q, r, s)$, the following transformations are obeyed by Pauli operators:

$$\begin{aligned} I \otimes \sigma_1 &\mapsto r_1 s_1 I \otimes \sigma_1 + r_2 s_1 \sigma_2 \otimes \sigma_3 \\ &\quad - r_1 s_2 \sigma_3 \otimes \sigma_2 + r_2 s_2 \sigma_1 \otimes I, \end{aligned} \quad (3.9)$$

$$\begin{aligned} I \otimes \sigma_2 &\mapsto s_1 q_1 I \otimes \sigma_2 + s_2 q_1 \sigma_3 \otimes \sigma_1 \\ &\quad - s_1 q_2 \sigma_1 \otimes \sigma_3 + s_2 q_2 \sigma_2 \otimes I, \end{aligned} \quad (3.10)$$

$$\begin{aligned} I \otimes \sigma_3 &\mapsto q_1 r_1 I \otimes \sigma_3 + q_2 r_1 \sigma_1 \otimes \sigma_2 \\ &\quad - q_1 r_2 \sigma_2 \otimes \sigma_1 + q_2 r_2 \sigma_3 \otimes I, \end{aligned} \quad (3.11)$$

where $q_1 = \cos(2q)$, $q_2 = \sin(2q)$, and similar expressions hold for r_1, r_2 , and s_1, s_2 , respectively.

The idea is now to evaluate $U^{\otimes t,t}|I\omega\rangle\rangle$ term by term in the expansion for $|\omega\rangle\rangle$, that is, we evaluate

$$\begin{aligned} U^{\otimes t}(I \otimes \omega) U^{\dagger \otimes t} &= \sum_{\nu} c_{\nu} U^{\otimes t} (I^1 \otimes \sigma_{\nu_1}^1 \dots I^t \otimes \sigma_{\nu_t}^t) U^{\dagger \otimes t} \\ &= \sum_{\nu} c_{\nu} \bigotimes_{i=1}^t U(I^i \otimes \sigma_{\nu_i}^i) U^{\dagger}, \end{aligned}$$

where now the transformation rules in Eq. (3.9)-(3.11) may be applied to each of the t factors independently. Computing the matrix element $\langle\langle I\omega|U^{\otimes t,t}|I\omega\rangle\rangle$, there is a contribution of the form $|c_{\nu}|^2 x^{p_1} y^{p_2} z^{p_3}$, arising from each of the terms $c_{\nu} I^1 \otimes \sigma_{\nu_1}^1 \dots I^t \otimes \sigma_{\nu_t}^t$, where $x = r_1 s_1$, $y = s_1 q_1$, $z = q_1 r_1$, and p_1, p_2, p_3 are the number of instances where $\nu_i = 1, 2, 3$, respectively. Summing over all terms in the expansion for $|\omega\rangle\rangle$ finally results in a polynomial of the form stipulated in Eq. (3.8), with $w_{\vec{p}} = \sum_{\nu} |c_{\nu}|^2$ determined by the sum over all strings ν that share the same \vec{p} -vector. That the polynomial is symmetric under the interchange of x, y , and z follows from the invariance of $|\omega\rangle\rangle$ under $U(2)$. Note that by construction, x, y , and z are bounded between $[-1, 1]$.

Let the degree of a Pauli string be the number of instances where $\nu_i \neq 0$. Since, under $U^{\otimes t}$ with $U \in U(2)$, a Pauli string can only be mapped to a Pauli string of equal degree, it follows that any $U(2)$ invariant whose expansion contains terms of differing degree can be written as a linear combination of $U(2)$ invariants each containing only terms of equal degree. For $t = 1$, the only $U(2)$ invariant is the identity. For $t = 2$, there is exactly one $U(2)$ invariant orthogonal to the identity, namely, $\omega = \frac{1}{\sqrt{3}}(\sigma_1^1 \sigma_1^2 + \sigma_2^1 \sigma_2^2 + \sigma_3^1 \sigma_3^2)$. Consequently, no $U(2)$ invariant contains a term of degree 1, and the only degree-2 terms a $U(2)$ invariant may contain are linear combinations of the form $\sigma_1^i \sigma_1^j + \sigma_2^i \sigma_2^j + \sigma_3^i \sigma_3^j$. Thus, for a monomial occurring in $\sum_{\vec{p}} w_{\vec{p}} x^{p_1} y^{p_2} z^{p_3}$, $2 \leq p_1 + p_2 + p_3 \leq t$, and if $p_1 + p_2 + p_3 = 2$, then exactly one of p_1, p_2 , or $p_3 = 2$.

The next step to establish the claimed result is to show that $\sum_{\vec{p}} w_{\vec{p}} x^{p_1} y^{p_2} z^{p_3} \leq \frac{1}{3}(x^2 + y^2 + z^2)$, where the right hand side is the polynomial corresponding to $\langle\langle I\omega_2|U^{\otimes t,t}|I\omega_2\rangle\rangle$, where $|\omega_2\rangle\rangle$ is any degree-2 $U(2)$ invariant. To show this we first show that the average over each set of monomials $x^{p_1} y^{p_2} z^{p_3}$ defined by a set of integers $p \geq p' \geq p''$ distributed in every distinct way to p_1, p_2 , and p_3 , is less than or equal to $\frac{1}{3}(x^2 + y^2 + z^2)$. There are two cases to consider:

- (i) If $p \geq 2$, then from $|x|, |y|, |z| \leq 1$, it follows that $x^{p \frac{1}{2}} (y^{p'} z^{p''} + y^{p''} z^{p'}) \leq x^2$, $y^{p \frac{1}{2}} (z^{p'} x^{p''} +$

$z^{p''} x^{p'}$ $\leq y^2$, and $z^{p'} \frac{1}{2}(x^{p'} y^{p''} + x^{p''} y^{p'}) \leq z^2$. Thus, the average of the left hand side of each inequality, which is the average over the desired set of monomials, must be less than or equal to the average of the right hand sides, which is $\frac{1}{3}(x^2 + y^2 + z^2)$.

(ii) If $p = p' = p'' = 1$, then using $x = r_1 s_1$, $y = s_1 q_1$ and $z = q_1 r_1$, $xyz \leq \frac{1}{3}(x^2 + y^2 + z^2)$ can be written $q_1^2 r_1^2 s_1^2 \leq \frac{1}{3}(r_1^2 s_1^2 + s_1^2 q_1^2 + q_1^2 r_1^2)$, which follows from $q_1^2 r_1^2 s_1^2 \leq r_1^2 s_1^2, s_1^2 q_1^2, q_1^2 r_1^2$.

Since $\sum_{\bar{p}} w_{\bar{p}} x^{p_1} y^{p_2} z^{p_3}$ is a weighted average of the above monomial averages, each of which is less than or equal to $\frac{1}{3}(x^2 + y^2 + z^2)$, it follows that $\sum_{\bar{p}} w_{\bar{p}} x^{p_1} y^{p_2} z^{p_3} \leq \frac{1}{3}(x^2 + y^2 + z^2)$.

Finally, the steps described above can be applied to the exchange term $\langle\langle I\omega|U^{\otimes t,t}|\omega I\rangle\rangle$, resulting in $\langle\langle I\omega|U^{\otimes t,t}|\omega I\rangle\rangle \leq \frac{1}{3}(x^2 + y^2 + z^2)$, where $x = b_2 c_2$, $y = a_2 c_2$, $z = a_2 b_2$ for any $U \in U(4)$. Since these inequalities hold for every $U \in U(4)$, it follows that

$$\begin{aligned} \langle\langle I\omega|m_t|I\omega\rangle\rangle + \langle\langle I\omega|m_t|\omega I\rangle\rangle \\ \leq \langle\langle I\omega_2|m_t|I\omega_2\rangle\rangle + \langle\langle I\omega_2|m_t|\omega_2 I\rangle\rangle, \end{aligned}$$

where $|\omega_2\rangle$ is any degree-2 $U(2)$ invariant. Since $\langle\langle I\omega_2|U^{\otimes t,t}|I\omega_2\rangle\rangle = \frac{1}{3}(x^2 + y^2 + z^2)$ (and the equivalent expression for $\langle\langle I\omega_2|U^{\otimes t,t}|\omega_2 I\rangle\rangle$) holds for every degree-2 $U(2)$ invariant, and the expression does not depend on t , it follows that the maximum of $\langle\langle I\omega|m_t|I\omega\rangle\rangle + \langle\langle I\omega|m_t|\omega I\rangle\rangle$ over all $|\omega\rangle$ such that $\langle\langle \omega|I\rangle\rangle = 0$ is given by $\langle\langle I\omega_2|m_2|I\omega_2\rangle\rangle + \langle\langle I\omega_2|m_2|\omega_2 I\rangle\rangle$. This concludes the proof. ■

3.3.1 Example: Haar measure on $U(4)$

As an example the case of $t = 2$ with $\tilde{\mu}(U)$ as the Haar measure on $U(4)$. The invariant eigenspace \mathcal{V}_2 of M_2 is spanned by the identity,

$$|I^{(n)}\rangle\rangle = (|I\rangle\rangle)^{\otimes n},$$

and the permutation

$$|S^{(n)}\rangle\rangle = (|S\rangle\rangle)^{\otimes n}$$

that swaps the $t = 2$ copies of $\mathcal{H} = \mathcal{H}_q^{\otimes n}$. Since $\tilde{\mu}(U)$ is the Haar measure, m_2 coincides with the projector onto the subspace \mathcal{V}_2 for $n = 2$ qubits. To find the excitation energies, we choose one of

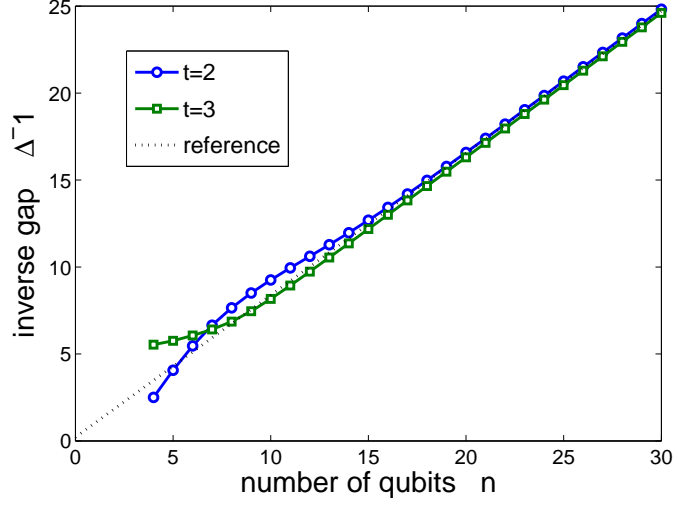


Figure 3.2: Inverse spectral gap Δ_t^{-1} of $M_t[\mu_H]$ with $t = 2, 3$ for a random circuit consisting of two-qubit gates selected according to the Haar measure on $U(4)$. The line with slope $5/6$ corresponds to the asymptotic result. From [19].

the extremal local kets, $|I\rangle\rangle$, and minimize

$$E_{\min} = 2 \min(1 - \langle\langle I\alpha|m_2|I\alpha\rangle\rangle - \langle\langle I\alpha|m_2|\alpha I\rangle\rangle),$$

over all local operators $|\alpha\rangle\rangle \in \mathcal{H}_t$ orthogonal to $|I\rangle\rangle$. This yields

$$|\alpha\rangle\rangle = |S\rangle\rangle - \langle\langle S|I\rangle\rangle|I\rangle\rangle = \sigma_1^1\sigma_1^2 + \sigma_2^1\sigma_2^2 + \sigma_3^1\sigma_3^2,$$

and $\Delta_t = 6/5n + \mathcal{O}(1/n^2)$. To determine how quickly the large- n scaling sets in, the fully symmetric sector of $M_t[\mu]$ under \mathcal{S}_n was numerically diagonalized. Since $\mu_H(U)$ is invariant under $U(2) \times U(2)$ transformations, \mathcal{H}_t may be restricted to the subspace of $SU(2)$ invariants. From angular momentum theory [21], the number of such invariants is

$$\sum_J m_J^2 = \frac{(2t)!}{(t+1)!t!} = C_t,$$

where m_J is the multiplicity of the $SU(2)$ -irrep with angular momentum J . Thus the dimension of the completely symmetric irrep of $M_t[\mu]$ may be taken to be $\binom{C_t+n-1}{n} \ll \binom{4^t+n-1}{n}$, which makes

numerical comparisons tractable for small t . Exact results for $t=2$ and 3 (see Fig. 3.2) indicate that the scaling prediction for Δ_t becomes very accurate for $n \gtrsim 14$.

3.4 Convergence of Random Quantum Circuits vs. Typical Gate Complexity

In this section I will examine some issues relating the quantum gate complexity of typical n -qubit unitary transformations to the scaling of the gap Δ_t of the t -order moment matrix. A reasonable conjecture based on the results for permutation invariant random quantum circuits is that $\Delta_t \geq \frac{a_t}{n}$. The question that I would like to address is whether or not this scaling conjecture is consistent with the fact that given a $U \in U(2^n)$ and an $\epsilon > 0$, in order to perform a unitary transformation $U' = U_k \dots U_1$ which is decomposable into k -single and two-qubit gates such that $\|U - U'\| < \epsilon$ requires $k = \mathcal{O}(n^2 4^n \log^c(n^2 4^n / \epsilon))$ [30].

Since for every irrep of $U(N)$ labeled s , there is a moment superoperator $M_t[\mu]$ such that s is one of the irreps that M_t can be decomposed into, it follows that a condition on each of the gaps Δ_t is a condition on each of the irreps of $U(N)$. That is, if $\Delta_t < \frac{a_t}{n}$ then $\|f^s\| < \frac{a_s}{n}$, where $d\mu_k(U) = \sum_{s=0}^{\infty} (f^s)^k D^s(U)$ is the Peter-Weyl expansion of the density $d\mu(U)$ corresponding to μ . Since the expansion for the Haar measure density $d\mu_H(U)$ is given by $f^0 = 1$ and $f^s = 0 \forall s > 0$, then for any density $d\mu_k(U)$, the l_2 norm of the difference between $d\mu_H(U)$ and $d\mu_k(U)$ is given by

$$\|d\mu_H(U) - d\mu_k(U)\|_2 = \int (d\mu_H(U) - d\mu_k(U))^2 = \sum_{s=1}^{\infty} \text{tr}((f^s)^2).$$

If for the largest eigenvalue of $(f^s)^2$, $\lambda_s < \frac{a_s}{n}$, then it follows that

$$\|d\mu_H(U) - d\mu_k(U)\|_2 < \frac{1}{n} \sum_{s=1}^{\infty} a_s^k.$$

Now if a_s does not depend on s , then $\|d\mu_H(U) - d\mu_k(U)\|_2$ can be made small for circuit length $k = \mathcal{O}(n)$. If in addition $d\mu_k(U)$ is continuous, then since $\|d\mu_H(U) - d\mu_k(U)\|_1 > \|d\mu_H(U) - d\mu_k(U)\|_2$, it follows that $\|\mu_H - \mu_k\|_{TV} = \|d\mu_H(U) - d\mu_k(U)\|_1$ can be made small for $k = \mathcal{O}(n)$. This would

force a contradiction, because this would imply that circuits of polynomial length in n are dense in $U(2^n)$.

There are two possibilities for avoiding this contradiction. Either a_s *must depend on* s in such a way that $\sum_{s=1}^{\infty} a_s^k$ remains large, or $d\mu_k(U)$ is *not* continuous. Interestingly, even if the two-qubit gate distribution $\tilde{\mu}$ is continuous, $d\mu_k(U)$ cannot be continuous for $k < 4^n$ since there are insufficient parameters in circuit of that length in order to parameterize all of $U(2^n)$, since $U(2^n)$ is a topological space with 4^n dimensions. A circuit with $k < k_d$ at best describes a surface in $U(N)$ with lower dimension and hence of measure zero in $U(N)$. Thus, for continuous $\tilde{\mu}$ one possibility is that the a_s do not depend on s , but since $d\mu_k(U)$ is not continuous until k is very large, the total variation distance remains near its maximum of 1 until $k = \mathcal{O}(n^2 4^n \log^c(n^2 4^n / \epsilon))$, at which point rapid convergence to the Haar measure occurs. Thus random quantum circuits may exhibit the so-called cut-off phenomenon [31].

Chapter 4

Irreversible Random Quantum Circuits

In this chapter the condition of invariance of the measure μ under Hermitian conjugation is relaxed, resulting in a moment superoperator $M_t[\mu]$ that is not Hermitian. For such operators $M_t[\mu]$, the gap defined by the spectral norm $\Gamma_{sp} \equiv \|M_t[\mu] - M_t[\mu_H]\|_{sp}$ is no longer a tight bound on the convergence rate. This possibility allows for random quantum circuits which may have faster convergence than the optimal reversible random quantum circuits discussed in Ch.3. The analysis will be limited to convergence of second order moments. Following [32, 33], under certain conditions on the distribution $\tilde{\mu}$ the evolution of the second order moments as a function of circuit depth can be mapped to a classical Markov chain. To obtain the mapping, the transformation $A_\alpha \rightarrow UA_\alpha U^\dagger$ induced by $U \in U(N)$, on an orthonormal basis of Hermitian observables $\{A_\alpha\}$ on \mathcal{H} . The transformation may be expressed as

$$A'_\alpha = \sum_\beta x_{\alpha\beta} A_\beta,$$

where $x_{\alpha\beta}(U) \in \mathbb{R}$ and $\sum_\beta x_{\alpha\beta}(U)x_{\gamma\beta}(U) = \delta_{\alpha\gamma}$. One may obtain the transformation of second order moments from the tensor

$$M_2[\mu]_{\alpha\beta\gamma\delta} = \int d\mu(U)x_{\alpha\beta}(U)x_{\gamma\delta}(U).$$

Whenever μ is such that,

$$M_2[\mu]_{\alpha\beta\gamma\delta} = 0, \text{ for } \alpha \neq \gamma, \beta \neq \delta, \quad (4.1)$$

it follows from orthonormality, that $\sum_{\beta} M_2[\mu]_{\alpha\beta\alpha\beta} = 1$ and $\sum_{\alpha} M_2[\mu]_{\alpha\beta\alpha\beta} = 1$, with each $M_2[\mu]_{\alpha\beta\alpha\beta} \geq 0$. Thus, the set of matrix elements $M_{\alpha\beta}[\mu] \equiv M_2[\mu]_{\alpha\beta\alpha\beta}$ is bistochastic, and hence defines the transition matrix M for a Markov chain on the state space labeled by α . If μ is reversible then in addition M is Hermitian. For the random quantum circuits that will be considered subsequently, the generalized Pauli basis will be used, and the state space of the corresponding Markov chain consists of strings from $\mathcal{J} = \{I, X, Y, Z\}^n$. The Markov matrix $M[\mu]$ will not be ergodic since there are 2 invariant vectors of the moment superoperator $M_2[\mu]$. But since one of the invariant vectors is given by the state I^n , the chain $M[\mu] - I^n$ is ergodic if μ is universal. If the random quantum circuit is irreversible, the asymptotic convergence of $M[\mu]$ to the remaining invariant vector can be upper bounded by $Ck^{J-1}(\lambda_*)^{k-J+1}$, where C is a constant depending on the initial state of the chain, J is the size of the largest Jordan block of $M[\mu]$, λ_* is the maximum square modulus of the eigenvalues of $M[\mu]$ [34]. Only if $J = 1$, implying that the random quantum circuit is diagonalizable, is the asymptotic decay a pure exponential.

4.1 Markov Chain Reduction

The full Markov chain M on the state space $\mathcal{J} = \{I, X, Y, Z\}^n$ may sometimes be reduced to a simpler chain M' , by partition the state space, \mathcal{J} , into subsets, $\mathcal{J}_a \subset \mathcal{J}$. A necessary and sufficient condition for reducing the chain is that the sum of the transition probabilities from an element of a subset, $a \in \mathcal{J}_a$, to all elements of any subset, $b \in \mathcal{J}_b$, is the same for each element of a , that is, $\sum_{u,v \in \mathcal{J}_b} M_{uv} = M_{ab}$ must be the same for all $u \in \mathcal{J}_a$ and all subsets \mathcal{J}_b . There are two cases in which this arises. The first is when the reduction removes a set of vectors that have eigenvalue 0 under M . In a Markov chain, this is equivalent to a complete loss of memory over some subsets of the state space. The second occurs when the Markov chain possesses a conserved quantity. In this case the chain, though irreducible, can be block diagonalized, (under a transformation which is not a permutation) so that at least one block, e.g. zero momentum for translational symmetry, is the desired reduced chain. Here, nontrivial eigenvalues that occur in M are absent in M' , and an additional argument

is needed to show that the subdominant eigenvalue does not occur in the remaining blocks.

If the random quantum circuit is *locally invariant*, then one may average over those Pauli strings that are equivalent under interchange of X , Y , or Z . The *local* reduced state is given by $P_i = X_i + Y_i + Z_i$, and the reduced state space consists of strings $\{I, P\}^n$. It will also be desirable to form reduced chains that average over only X and Y local Pauli operators by defining the new local variables $\Xi_i^\pm = X_i \pm Y_i$ so that chain states now consist of the set $\{I, Z, \Xi\}^n$.

A Markov chain can admit a reduced chain of the second type by forming equivalence classes of Pauli operators under permutation symmetry. In the case of full permutation symmetry, since equivalence classes may be labeled by how many X , Y , and Z 's are in each Pauli operator, or the appropriate symbols for locally reduced chains, the size of the reduced state space grows only polynomially in the number of qubits n , allowing scaling behavior of Markov matrix properties with circuit size to be determined numerically. Note that while the reduced representation formed due to local invariance contains every non-zero eigenvalue in the full Markov chain, reduced representations induced by qubit permutations discard eigenvalues associated with asymmetry with respect to the permutations.

4.2 Parallel Random Quantum Circuits and Cluster States

The first irreversible random quantum circuit to be considered is the circuit proposed in [11] which consists of independent Haar random single qubit gates on each qubit, followed by performing controlled-phase gates, $CZ = |0\rangle\langle 0| \otimes J + |1\rangle\langle 1| \otimes Z$, between nearest neighbors on an open chain. Although the single qubit gates are selected independently from a reversible distribution, the subsequent CZ gates break reversibility. Furthermore, since this circuit involves parallel operations, it may be naturally implemented as a measurement pattern on a cluster state.

Cluster states are highly entangled states which serve as the basic resource for measurement-based quantum computation [35]. They may be generated by applying CZ gates between qubits initially in the $|+\rangle$ state. Computation is executed by measuring qubits along desired axes in the x - y plane. The choice of measurement axis determines the operation that is implemented, and may depend on the outcome of a previous measurement. A 2D qubit lattice with CZ gates applied between

all nearest neighbors suffices for universal quantum computation. Measurements are performed by column from left to right, until a last column is left unmeasured – determining the statistics over the computation outcomes.

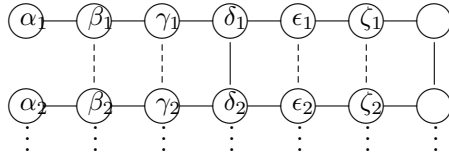


Figure 4.1: Schematics of cluster-state PR architectures. Pairs of qubits subjected to CZ gates are connected by solid lines and each qubit is identified by the angle in the x - y plane that defines its measurement basis. Dashed lines represent additional CZ gates for the enhanced version of the algorithm from [11].

A cluster state architecture that implements the equivalent of 2 iterations of the PR algorithm of [11] is depicted in Fig. 4.1. Using Euler-angle representation, measurement of 3 qubits in a row simulates a single-qubit gate $HZ(\alpha_i + \pi m_{\alpha_i})X(\beta_i + \pi m_{\beta_i})Z(\gamma_i + \pi m_{\gamma_i})$, where H is the Hadamard gate, $Z(\alpha)$ ($X(\alpha)$) is a z - (x -) rotation by an angle α , $(\alpha_i, \beta_i, \gamma_i)$ are the angles along which each qubit is measured in the x - y plane, and $m_i = 0, 1$ labels additional measurement-dependent π rotations. Arbitrary single-qubit gates are effected by properly choosing the Euler angles. Because the Haar measure on $SU(2)$ is invariant under the extra π rotations, the latter may be ignored. CZ gates performed between rows of the cluster state (vertical lines) serve as CZ gates acting between qubits in the circuit-based algorithm. In general, to simulate ℓ iterations of an n -qubit PR circuit, a lattice of $n \times 3\ell + 1$ qubits is needed (where the extra 1 comes from the final, unmeasured column). The first column contains the initial state $|\psi_0\rangle$ on which the algorithm operates.

Given the measurement pattern of Fig. 4.1, a natural question arises: Can the convergence rate of the cluster-state PR algorithm be enhanced by filling in *additional* vertical lines (that is, by effecting additional CZ gates represented by dashed lines)? In this case, the computation proceeds as before but measurement angles will be chosen randomly in the x - y plane. Fig. 4.2 illustrates the resulting improvement by comparing the decay rate with respect to two measures of convergence

1. The l_2 distance between the distribution of squared moduli of the components of the final state, $P(y)$, and the Porter-Thomas distribution $P_{PT}(y) = \exp(-y)$ where $y = N\nu$ and $N = 2^n$, which describes the distribution of Haar random states.

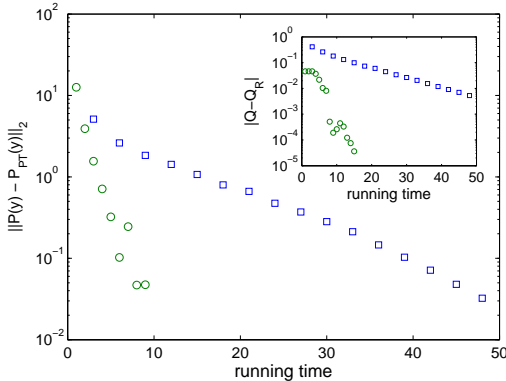


Figure 4.2: Distance of the (normalized) distribution of squared moduli state-vector components from $P_{PT}(y)$ for random states as a function of run time. \square : Standard (6 rows and connections every third column), vs \circ : Enhanced (connections at every column) PR patterns. The run time equals the number of columns in the cluster state. Inset: Difference of global entanglement, Q , from the expected random-state value, Q_R , vs run time. For both test functions, the enhanced version of the algorithm converges to the Haar average with a rate about 6 times faster.

2. The difference between the Meyer-Wallach entanglement [82]

$$Q = 1 - \frac{1}{n} \sum_{i=1}^n \sum_{\alpha=x,y,x} \langle \psi | \sigma_{\alpha}^i | \psi \rangle^2,$$

from its expectation for Haar random states.

For 6 row cluster states, both test functions converge approximately 6 times faster for the completely filled cluster state. Thus, the enhanced version of the PR cluster-state algorithm uses a factor of 6 fewer qubits and horizontal connections, and half the number of vertical connections to achieve a comparable distance from random-state behavior.

Because the cluster model is computationally equivalent to the circuit model [35], the improved measurement pattern for the enhanced cluster-state PR algorithm must have a circuit model analog. The single-qubit rotation equivalent to measuring a cluster qubit in a random basis in the x - y plane is an $HZ(\alpha)$ gate. Thus, once translated into the circuit model, the completely filled measurement pattern identifies a *restricted* family of random single-qubit gates which map the z -axis to the transverse plane. In the circuit model, the decay rate of the enhanced algorithm is only about 2 times faster, since a time step counts as a complete iteration. Still, depending on implementation, it

may be easier to perform an $HZ(\alpha)$ gate than an arbitrary single-qubit gate. This raises the following general question: Given a *fixed* two-qubit gate, what is the *optimal* single-qubit gate distribution to employ?

Since the z -axis is fixed by the CZ gates only gate distributions which are invariant under rotations about the z -axis will be considered. Thus, the Markov chain corresponding to the single-qubit gate distribution will consist of I, Z, Ξ with $\Xi = X+Y$. All such single, qubit gate distribution, for which a Markov chain representation exists may be fully parameterized as follows

$$R(c) = \begin{pmatrix} 1 & 0 & 0 \\ 0 & c & \frac{1-c}{2} \\ 0 & 1-c & \frac{1+c}{2} \end{pmatrix}.$$

If a single-qubit gate is selected independently for each qubit, and applied in parallel, then the corresponding local part of the Markov chain $L(c) = R(c)^{\otimes n}$. The subsequent CZ gates act as a permutation on the state space $I, Z, \Xi^{\otimes n}$ corresponding to the full n -qubit circuit. This permutation acting on $L(c)$, yields the transition matrix $M(c)$. Numerically we find that $M(c)$ though non-Hermitian is diagonalizable, that is each Jordan block is of dimension one, thus the convergence is asymptotically exponential, with a rate $\Gamma(c)$ determined by the gap between the largest eigenvalue of 1 and absolute value of the second largest eigenvalue, $\Delta(c) = 1 - |\lambda_1|$, via $\Gamma(c) = -\ln(1 - \Delta(c))$. Thus, the larger the gap the faster the convergence. Here, we are interested in the gap between 1 and the next largest eigenvalue whose eigenvector has a non-zero component along $|\psi_0\rangle\langle\psi_0|$.

As seen in Fig. 4.3, the maximum gap for $n = 6$ qubits, equal to 0.4135, occurs at $c \approx 0.03$. The gap for $HZ(\alpha)$ gates, $\Delta(0) \approx 0.4071$, is significantly larger than the gap for random rotations, $\Delta(1/3) \simeq 0.2292$, yielding $\Gamma(0)/\Gamma(1/3) \approx 2.008$. For $n = 10$, the maximum gap is attained at $c = 0$. Remarkably, as n increases, Δ *decreases* for unrestricted local gates, but *increases* for $HZ(\alpha)$ gates, see inset of Fig. 4.3. Thus, the larger n , the faster the Markov chain converges.

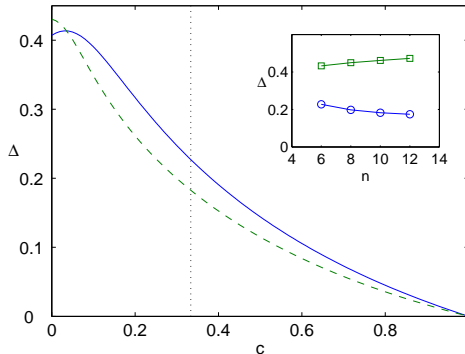


Figure 4.3: Gap, $\Delta(c)$, between the largest eigenvalue of 1 and the absolute value of the largest non-unit eigenvalue of $M(c)$ vs c , for $n = 6$ (solid line) and $n = 10$ (dashed line). The gap at $c = 0$ ($HZ(\alpha)$ gates) is significantly larger than the gap at $c = 1/3$ (arbitrary random single-qubit gates), identifying the optimal gate set. Inset: Gap for $c = 1/3$ (circles) and $c = 0$ (squares) vs n .

4.3 Permutationally Invariant Random Quantum Circuits

Since the single qubit gate distribution parameterized by $HZ(\alpha)$ where $\alpha \in [0, 2\pi]$ generates a faster convergence rate than Haar random single qubit gates in the above random quantum circuit design, is interesting to see if this enhancement occurs for other random quantum circuit formats. A thorough exploration of different random quantum circuit design parameters is given in [36], and the specific case of permutation invariant random quantum circuits will be discussed here.

The second order moments of permutationally invariant *reversible* random quantum circuits that can be expressed in terms of an appropriate reduced Markov chain, before generalizing to *irreversible* permutation invariant random quantum circuits.

Given a two-qubit gate distribution $\tilde{\mu}$ that satisfies Eq.(4.1), there is a 16×16 bistochastic matrix $M[\mu]$ describing the evolution of the non-vanishing second order moments of $\tilde{\mu}$ corresponding Pauli strings of length 2. If $\tilde{\mu}$ is locally invariant, then only a 4×4 transformation matrix is required to indicate transitions within the state space $\{I, P\}^2$. For the Haar measure on $U(4)$, every 2 qubit Pauli operator is equally likely to be mapped to any other 2 qubit Pauli operator. Since there are 3

Pauli operators in the reduced class PI and IP and 9 in PP this yields,

$$m[\tilde{\mu}_H] = \begin{pmatrix} 1 & 0 & 0 & 0 \\ 0 & 1/5 & 1/5 & 1/5 \\ 0 & 1/5 & 1/5 & 1/5 \\ 0 & 3/5 & 3/5 & 3/5 \end{pmatrix}.$$

As described above, because of permutation symmetry the chain may be reduced further, so that the state space is labeled only by the number of Pauli operators, n_P , in each Pauli string. When the bi-local gate distribution is the Haar measure, the transitions between the first three states $n_P = 1, 2,$ and 3 are given below:

$$M[\tilde{\mu}_H] = \begin{pmatrix} 1 - 2/5n & 9/4n^2 & 0 \\ 2/5n & 1 - 4/5n - 9/4n^2 & 11/4n^2 \\ 0 & 4/5n & 1 - 8/5n - 11/4n^2 \end{pmatrix}.$$

As $n \rightarrow \infty$, the off-diagonal elements on the upper right go to zero compared to the spacings between the respective diagonal matrix elements, thus $M[\tilde{\mu}_H]$ becomes approximately a lower triangular matrix, suggesting that as $n \rightarrow \infty$ the eigenvalues are given by the diagonal matrix elements. Now consider the eigenvalue equation,

$$\begin{pmatrix} 1 - 2/5n & 9/4n^2 & 0 \\ 2/5n & 1 - 4/5n - 9/4n^2 & 11/4n^2 \\ 0 & 4/5n & 1 - 8/5n - 11/4n^2 \end{pmatrix} \begin{pmatrix} x_1 \\ x_2 \\ x_3 \end{pmatrix} = \lambda \begin{pmatrix} x_1 \\ x_2 \\ x_3 \end{pmatrix}.$$

Assuming that $\lambda = 1 - \sum_{l=1}^{\infty} \frac{a_l}{n^l}$ and $x_i = 1 + \sum_{l=1}^{\infty} \frac{b_l^i}{n^l}$, the eigenvalue equation can be solved to each order in n . To order $1/n$, each eigenvalue is given by the a diagonal matrix elements. This method is equivalent to the mean-field Ansatz of bosonic excitations discussed in Ch.3. Although it is not obvious in this form, the eigenvalues that approach 1 as $n \rightarrow \infty$ are nearly 2-fold degenerate, with a splitting that decreases exponentially with n as described in Eq.(3.7).

Setting $c = 0$ in Eq.(4.2) yields the Markov matrix $R(0)$ corresponding to the single qubit gate distribution $HZ(\alpha)$ with α selected uniformly from $[0, 2\pi]$. Taking $R(0) \otimes R(0)$ and appropriately

permuting the elements of $\{I, Z, \Xi\}^2$ under the action of CZ , yields the following bi-local Markov matrix:

$$m[\tilde{\mu}_{HZ}] = \begin{pmatrix} 1 & 0 & 0 & 0 & 0 & 0 & 0 & 0 & 0 \\ 0 & 0 & 1/2 & 0 & 0 & 0 & 0 & 0 & 0 \\ 0 & 0 & 0 & 0 & 0 & 0 & 0 & 0 & 1/4 \\ 0 & 0 & 0 & 0 & 0 & 0 & 1/2 & 0 & 0 \\ 0 & 0 & 0 & 0 & 0 & 0 & 0 & 0 & 1/4 \\ 0 & 1 & 1/2 & 0 & 0 & 0 & 0 & 1/2 & 0 \\ 0 & 0 & 0 & 0 & 0 & 0 & 0 & 0 & 1/4 \\ 0 & 0 & 0 & 1 & 0 & 1/2 & 1/2 & 0 & 0 \\ 0 & 0 & 0 & 0 & 1 & 1/2 & 0 & 1/2 & 0 \end{pmatrix}$$

Because of permutation symmetry, a further reduction can be performed resulting in a Markov chain on a state space labeled with only the number (n_z, n_ξ) of Z or Ξ symbols occurring in any Pauli string. The gap is controlled by the transitions between the states with the first three lowest values of $n_z + n_\xi$, $(1,0)$, $(0,1)$, and $(1,1)$ shown below:

$$M[\tilde{\mu}_{HZ}] = \begin{pmatrix} 1 - 2/n & 1/n & 0 \\ 0 & 1 - 2/n & 4/3n^2 \\ 2/n & 1/n & 1 - 4/n - 4/3n^2 \end{pmatrix}.$$

An expansion similar to that used to diagonalize the previous chain can be used to diagonalize $M[\tilde{\mu}_{HZ}]$. The eigenvalues that are 1 to leading order are similarly given by the diagonal matrix elements, however, the transition of order $1/n$ between $(1,0)$ and $(0,1)$ introduces corrections on higher order term of $1/(n\sqrt{n})$ rather than $1/n^2$ as in the case of the previous circuit. This chain may be diagonalized numerically for large enough n to confirm the validity of the above Ansatz. Note that for random quantum circuits consisting of independently selected single and two-qubit gates, as considered here, the asymptotic decay rate to the Haar measure is limited by the transitions from Pauli strings containing only one Pauli operator to those containing two. For reversible random quantum circuits, there is always a probability that even if the qubit corresponding to the single Pauli operator is chosen, the Pauli operator will be left unchanged. Since the probability of choosing

any given qubit with a two qubit gate is $2/n$, the convergence rate of $1 - 2/n$ is optimal for such random quantum circuits and can be achieved by the above irreversible random quantum circuit.

Chapter 5

Quantum Chaos: Background

One way of loosely defining the concept of chaos is how apparently random dynamics can result from simple dynamical laws. In the case of classical systems this may be said to arise through the properties of the classical dynamical flow which can be expressed in terms of the Liouville equation,

$$\frac{\partial \rho}{\partial t} = -\frac{\partial H}{\partial q} \frac{\partial \rho}{\partial p} + \frac{\partial H}{\partial p} \frac{\partial \rho}{\partial q} \equiv -\{H, \rho\}_{PB},$$

and $\rho(q, p, t)$ is a phase space density and H is the system Hamiltonian. A flow is considered chaotic if it satisfies the following properties: the phase space trajectories display sensitivity to initial conditions, topological mixing occurs, and the periodic orbits are dense. By sensitivity to initial conditions, if there are two points in phase space that are arbitrarily close, then they separate at short time scales as $e^{\lambda t}$, where λ is the largest Lyapunov exponent. Topological mixing occurs when any two open subsets A and B of the phase space (q, p) eventually overlap [38, 39].

A classical dynamical system is said to be *integrable* if there exists a set of as many well-behaved functions $I_j(p, q)$ such that $\{H, I_j\}_{PB} = 0$ and $\{I_j, I_k\}_{PB} = \delta_{jk}$, and any two integrals of motion I_j and I_k are functionally independent, as there are degrees of freedom. The functions $I_j(p, q)$ are independent if and only if the differential elements $dI_i = \sum_j \frac{\partial I_i}{\partial q_j} dq_j + \frac{\partial I_i}{\partial p_j} dp_j$ are linearly independent for all values in phase space (q, p) . Since $\{H, I_j\}_{PB} = 0$, each integral I_j is constant of the motion. Since the integrals of motion are functionally independent, the surface formed by specifying

a constant value for any $I_i = c_i$, determines a family of tori, to which the dynamics is limited. There can be no sensitivity to initial conditions and no ergodicity since each trajectory is strictly limited to the torus on which it begins.

In quantum mechanics the dynamical flow on a complete set of phase space variables is replaced by a unitary transformation, $U = \exp(-iHt)$, generated by the quantum Hamiltonian H operator acting on a Hilbert space \mathcal{H} . If the classical phase space is bounded then the Hilbert space is countably infinite, and the Hamiltonian has a discrete set of eigenvalues $\{E_\alpha\}$. Since quantum position and momentum operators do not commute, one can not specify both with complete accuracy, and thus there is no direct quantum analog of the phase space trajectory. The most that can be known are the probabilities for a complete set of measurement outcomes, which can be expressed as a density operator $\hat{\rho}$, and is analogous to the classical phase space density.

Because of the correspondence principle, the question arose whether the behavior of quantum systems whose classical limits are chaotic is in any way different from the behavior of quantum systems whose classical limits are integrable. Due to the nature of unitary quantum evolution, it was doubtful that quantum systems could produce the standard dynamical criteria that define classical chaos, for example there can be no sensitivity to small changes in the initial wavefunction. This itself does not mean that quantum systems cannot exhibit chaos, since by Koopman's theorem [40], the overlap of any two classical phase space densities is also preserved under classical dynamics. Attempts have been made to find unifying criteria that are satisfied by both quantum and classical chaos. Sensitivity of the Hamiltonian to perturbations was put forth in [37, 41, 42]. Although this approach is valid in the classical limit, for systems such that a classical limit is not approached chaoticity can enhance stability [44, 45].

Nevertheless, for quantum systems, apparent stochastic time evolution can arise through statistical properties of the eigenvectors and eigenvalues of the quantum Hamiltonian [46, 47]. Specifically, there is considerable numerical evidence that the eigenvectors and eigenvalues of strongly non-integrable quantum Hamiltonians appear random within certain system specific constraints, where the fluctuations are of a universal form which is equivalent to those of ensembles of random matrices [48, 38, 49, 8, 18]. This mathematical phenomenon appears to be a property of typical diagonalization problems of Hermitian linear operators [52, 50], and thus arises in the normal modes of both

classical and quantum wave phenomena, scattering matrices, adjacency matrices of graphs, Markov chains, and even financial models [53]. Beyond linear diagonalization problems, it arises in other contexts, such as in connection to the zeros of the Riemann ζ -function and hence to the distribution of prime numbers [51] and other problems in number theory [52].

Despite the different origin, quantum (mode) chaos and classical (ray) chaos are non-trivially connected by the correspondence principle, since in the limit of small wavelengths, the quantum wave dynamics can be approximated by rays describing the classical trajectories. This semi-classical connection has been studied extensively, with particular emphasis on dynamical billiards [38]. Thus, mode chaos appears to be the analog of classical chaos in quantum systems, and will be what the term quantum chaos shall refer to herein. Since quantum chaos is a ubiquitous property of complicated linear diagonalization problems, it arises generally in quantum Hamiltonians, even in the absence of a natural classical limit, in particular, for many-body systems of interacting fermions, bosons, or localized spins. This section of the thesis will focus on quantum chaos in such many-body systems. Specifically, I will be interested in obtaining a description of the system specific constraints for quantum many-body systems, and a characterization of the fluctuations around these constraints. I will use these results to examine some properties of the many-body eigenvectors, and some properties of the time evolution. Before turning to quantum many-body systems I will briefly review the main results and conjectures for quantum systems that possess a classical limit which is chaotic.

5.1 Eigenvalue Statistics

Let $H(q, p)$ be a classical Hamiltonian with no explicit time dependence where q and p represent d generalized coordinates and momenta. One may quantize H by introducing Hermitian operators \hat{q} and \hat{p} , that act on a Hilbert space \mathcal{H} with commutation relations corresponding to the classical Poisson brackets between the generalized coordinates and properly symmetrizing products of \hat{q} and \hat{p} so that $H(\hat{q}, \hat{p})$ is Hermitian. If the classical phase space is compact then \mathcal{H} has a discrete basis, and $H(\hat{q}, \hat{p})$ has a discrete spectrum $\{E_\alpha\}$. If $H(q, p)$ is an increasing function of the momenta, p , then as $E \rightarrow \infty$ the de Broglie wavelength becomes sufficiently small so that the wave dynamics can be replaced by rays, which describe the classical trajectories.

Let $s(E) = \sum_{\alpha} \delta(E - E_{\alpha})$ be the density of states of $H(\hat{q}, \hat{p})$. When $s(E)$ is smoothed by averaging over an energy window containing a large number of levels, the density of states is governed by system specific details of the classical Hamiltonian $H(p, q)$. Specifically, in the high energy limit the smoothed quantum mechanical density of states is proportional to the corresponding volume of classical phase space [38, 48, 54],

$$\lim_{\epsilon \rightarrow 0} \lim_{E \rightarrow \infty} \frac{1}{\epsilon} \int_E^{E+\epsilon} dE s(E) = \frac{1}{(2\pi\hbar)^d} \int dpdq \delta(E - H(p, q)). \quad (5.1)$$

This result was first proved by Weyl [55] for the normal modes of the Laplacian on an irregular bounded domain, and the formula is referred to as Weyl's law, or the Thomas Thomas-Fermi density.

5.1.1 Bohigas-Gianonni-Schmidt conjecture

Weyl's law (5.1) for the smoothed density of states holds for both integrable and chaotic systems, however the level to level fluctuations of the density of states on energy scales much less than those at which the smoothed density varies depends on whether the classical system is chaotic or integrable. To characterize the short range fluctuations in the density of states, the spectrum must be rescaled $\{E_{\alpha}\} \rightarrow \{\tilde{E}_{\alpha}\}$ so that the smoothed density of states is everywhere equal to 1. The limit $\tilde{E} \rightarrow \infty$ can then be used to define a family of joint probability densities, $P_k(s_1, \dots, s_k) ds_1 \dots ds_k$ of finding the spacing $s_1 \dots s_k$ between sets of $k + 1$ consecutive eigenvalues. Bohigas, Gianonni and Schmidt [49] conjectured that if the classical Hamiltonian $H(q, p)$ is chaotic, then within the smoothly varying density the sequence of eigenvalues is pseudo-random with fluctuations between nearby eigenvalues equivalent to those of an ensemble of random Hermitian matrices that depends only on the symmetry class of the Hamiltonian. There are three such symmetry classes.

- **Gaussian Unitary Ensemble (GUE)** : In the absence of any global symmetry, the appropriate ensemble of Hermitian matrices is invariant under arbitrary unitary transformations. This is satisfied by the ensemble of $N \times N$ Hermitian matrices with each off-diagonal matrix elements an independent random complex numbers $a_{ji}^* = a_{ij} = x_{ij} + iy_{ij}$ such that each x_{ij} and y_{ij} with $i < j$ are independent Gaussian random variables with variance v . Each diagonal matrix element a_{ii} is an independent Gaussian random variable with variance $2v$.

- **Gaussian Orthogonal Ensemble (GOE)** : If the Hamiltonian is invariant under an anti-unitary transformation T , such that, $T^2 = 1$, then a basis may be constructed so that H has purely real matrix elements, without first obtaining detailed information about the eigenvectors of H . The most general basis transformations that preserve the realness of the matrix elements of H is the set of orthogonal transformations. An ensemble of Hermitian matrices invariant under arbitrary orthogonal transformation can be generated by selecting real matrix elements independently at random from a Gaussian distribution, such that the variance of the diagonal matrix elements is twice that of the off-diagonal matrix elements.

- **Gaussian Symplectic Ensemble (GSE)** : If the Hamiltonian is invariant under an anti-unitary transformation T such that $T^2 = -1$, and H has no other symmetries, then a basis may be constructed consisting of pairs, $|m\rangle \neq T|m\rangle = |m'\rangle$. Consider the 2×2 block of corresponding to two such pairs,

$$\begin{pmatrix} \langle l|H|m\rangle & \langle l|H|Tm\rangle \\ \langle Tl|H|m\rangle & \langle Tl|H|Tm\rangle \end{pmatrix}.$$

Invariance under T implies that each such block can be parameterized with real quaternions. The subgroup of $U(N)$ that preserves this parametrization is a representation of the symplectic group, and the corresponding Hermitian matrix ensemble consists of independent Gaussian random real quaternions [48].

Typically, the nearest neighbor level spacing distribution $P_1(s)ds$ is employed in numerical studies, however alternative measures such as the rigidity [38] or the variance of the number of rescaled energy levels in a given window are also used.

For each matrix ensemble the unfolded nearest neighbor level spacing distribution is distinct:

$$GOE : p(s)ds = \frac{\pi s}{2} e^{-\frac{\pi s^2}{4}} \quad (5.2)$$

$$GUE : p(s)ds = \frac{32s^2}{\pi^2} e^{-\frac{s^2}{\pi}} \quad (5.3)$$

$$GSU : p(s)ds = \frac{21^8 s^4}{3^6 \pi^3} e^{-\frac{64s^2}{9\pi}} \quad (5.4)$$

Random matrix predictions are only expected to hold on an energy scale that is much smaller

than the scale at which the smoothed density of states varies. If one lets $\hbar \rightarrow 0$, then the density of states in any energy window becomes infinite, and arbitrarily large rescaled energy widths are expected to conform to random matrix distributions.

5.2 Eigenvector Statistics

There are similar conjectures for the matrix elements $\langle \alpha | A(p, q) | \beta \rangle$ of a well-behaved observable A with respect to the eigenvectors $\{|\alpha\rangle\}$ of $H(\hat{p}, \hat{q})$. The first is that the average diagonal matrix element $\langle \alpha | A | \alpha \rangle$ over any finite energy window converges to the classical microcanonical average of the corresponding observable in the semiclassical limit, that is,

$$\lim_{\epsilon \rightarrow 0} \lim_{E \rightarrow \infty} \left[\frac{1}{N(E, \epsilon)} \sum_{\alpha: E < E_\alpha < E + \epsilon} \langle \alpha | A | \alpha \rangle \right] = \frac{\int dpdq A(p, q) \delta(E - H(p, q))}{\hbar^d s_{CL}(E)},$$

where $N(E, \epsilon) = \int_E^{E+\epsilon} dE s(E)$, where $s(E)$ denotes as before the density of states, and $s_{CL}(E) = \int dpdq \delta(E - H(p, q))$ is the *classical* density of states. This conjecture is referred to as the *local Weyl law* [56, 57].

It was conjectured by Feingold and Peres [58] that the “empirical” variance of off-diagonal matrix elements $\langle \alpha | A | \beta \rangle$ is determined by the frequency component of the classical auto-correlation function corresponding to the energy difference, $\omega = (E_\alpha - E_\beta)/\hbar$. The empirical variance may be defined as follows:

$$v(E, \omega; \epsilon_1, \epsilon_2) \equiv \left[\frac{1}{N(E, \epsilon_1)N(E + \hbar\omega, \epsilon_2)} \sum_{\substack{E < E_\alpha < E + \epsilon_1 \\ \hbar\omega < E_\alpha - E_\beta < \hbar\omega + \epsilon_2}} |\langle \alpha | A | \beta \rangle|^2 \right]. \quad (5.5)$$

In the high energy limit this is given by the Fourier transform of the classical auto-correlation function, that is,

$$\lim_{\epsilon_1, \epsilon_2 \rightarrow 0} \lim_{E \rightarrow \infty} v(E, \omega; \epsilon_1, \epsilon_2) = \frac{\tilde{C}_A(\omega)}{\hbar^d s_{CL}(E)},$$

where

$$\tilde{C}_A(\omega) = \int_{-\infty}^{\infty} C_A(\tau) e^{i\omega\tau} d\tau$$

and

$$C_A(\tau) = \lim_{T \rightarrow \infty} \frac{1}{T} \int_0^T A(q(t), p(t)) A(q(t + \tau), p(t + \tau)) dt$$

for any classical ergodic trajectory $(q(t), p(t))$. Feingold and Peres furthermore conjectured that the empirical variance of diagonal matrix elements,

$$v_D(E) = \frac{1}{N(E, \epsilon)} \sum_{E < E_\alpha < E + \epsilon} \left(\langle \alpha | A | \alpha \rangle - \overline{\langle \alpha | A | \alpha \rangle} \right)^2,$$

is proportional to the off-diagonal variance as the energy difference goes to zero by a factor c depending on the symmetry class of the Hamiltonian,

$$v_D(E) = c \frac{\tilde{C}_A(0)}{\hbar^d s_{CL}(E)}.$$

There is significant numerical support for the above conjectures [59]. It has been proved in [60], that for chaotic quantum billiards, the diagonal variance for well-behaved observables, goes to zero in the high energy limit, for all but a subsequence of eigenstates of measure zero. This result is known as the *quantum ergodicity theorem*.

Beyond the constraints on the averages of the diagonal matrix elements, and empirical variances of off-diagonal matrix elements, it is also conjectured [58] that the distribution of matrix elements is Gaussian in the high energy limit. This is related to the conjecture by Berry [61] that the eigenstates for chaotic billiards may be described by “random plane waves” of fixed wavevector, and is equivalent to the idea presented in [63] that the high energy eigenstates of systems with a chaotic classical limit ought to be as random as possible subject to prior constraints.

5.3 Integrability and Chaos in Quantum Many-Body Systems

It is not possible to directly borrow the notion of classical integrability and apply it to quantum systems with a finite dimensional Hilbert space. One may be tempted to define integrability for such systems as the existence of as many independent integrals of motion I_i that commute with

each other $[I_i, I_j] = 0$ and with the Hamiltonian $[H, I_i] = 0$, as degrees of freedom. The first problem with this definition is that for a quantum system with a finite dimensional Hilbert space, the number of degrees of freedom can be ambiguous, nor is it immediately clear in what sense the integrals of motion ought to be independent. One reasonable definition for independence of commuting observables is that specifying the eigenvalue of one observable does not constrain the allowed eigenvalues for an observable that is independent of it. This notion is equivalent to *algebraic independence*. A set $\{I_i\}$ of commuting observables are algebraically independent if and only if there does not exist a function f such that $f(I_1, \dots, I_n) = 0$ [64]. This definition implies that each observable I_i is degenerate, and that the degenerate eigenspaces of any two observables do not coincide. Furthermore, if the number of distinct sets of joint eigenvalues of the $\{I_i\}$ is equal to the dimension of the Hilbert space, then the set $\{I_i\}$ can be used to define a basis of \mathcal{H} and form a complete set of commuting observables. If each I_i has exactly d degenerate eigenspaces, and each of the eigenvalues is completely unconstrained by the eigenvalues of the others, then it follows that $\dim(\mathcal{H}) = d^n$, and one may define a tensor product factorization, $\mathcal{H} = \mathcal{H}_I^{\otimes n}$ so that each I_i acts on a separate factor space and may naturally be considered a degree of freedom equivalent to a subsystem [65]. The problem lies in the fact that for a fixed finite dimensional Hilbert space such observables always exist, unlike the case for classical systems, making a definition of quantum integrability that relies solely of the existence of such integrals of motions vacuous. The intuition regarding such integrals of motion still applies, if they may be determined *without* performing a full diagonalization of the Hamiltonian first. The existence of an efficient procedure, for specifying any particular eigenvector and eigenvalue, or the mathematical structure underlying such a procedure, plays roughly the same role for quantum many-body systems as the existence of a set of integrals of motion does in classical dynamics. Some examples of quantum integrable systems include those many-body Hamiltonians diagonalizable by Jordan-Wigner transformation [66, 67], generalized mean-field Hamiltonians efficiently diagonalizable by algebraic techniques, as well as those models diagonalizable by Bethe Ansatz or inverse scattering methods more generally. Though awaiting a fully rigorous definition, from an operational standpoint the existence of such simplifying mappings is the basic idea of quantum integrability.

As is the case for classical systems, no such simplifying structure is believed to exist for most

physically relevant quantum many-body Hamiltonians. For such non-integrable Hamiltonians, a complete description of a generic eigenvector and the corresponding eigenvalue requires an exponentially growing number of computational steps in terms of the the number of subsystems, although the extremal eigenvalues and eigenvectors may still be efficiently computable [68]. There is significant numerical and experimental evidence that the eigenvalues and eigenvectors of non-integrable many-body systems tend to display generic properties of random matrices and the use of random matrix methods has been applied extensively in nuclear physics [69, 70]. In the next chapters, a statistical description of high energy eigenvectors of non-integrable many-body systems will be constructed, and used to examine both properties of the eigenvectors such as entanglement content, and to understand some aspects of the dynamics generated by the Hamiltonian.

Chapter 6

Constraints on the Statistical Properties of Quantum Chaotic Many-Body Hamiltonians

In this chapter I shall focus on analyzing the statistical properties of the eigenvectors and eigenvalues of non-integrable many-body quantum Hamiltonians in the thermodynamic limit, whereby the number of subsystems $n \rightarrow \infty$. A method for determining the thermodynamic limit of the smoothed density of states, as well as the smoothed microcanonical expectation values and dynamical correlation functions for observables local to a fixed subsystem in the thermodynamic limit is presented. Building on earlier works [9, 71, 72, 73], the method employs an expansion in terms of a complete set of polynomials that are orthogonal with respect to the exact density of states. Notably, the limiting thermodynamic behavior of the above smoothed quantities is general for Hamiltonians consisting of two-body interactions between finite dimensional subsystems (qudits), *irrespective of whether the Hamiltonian is integrable or not*. The way in which the constraints are satisfied, however, will depend on whether the system is integrable. Specifically, strongly non-integrable Hamiltonians will tend to satisfy these constraints *uniformly with respect to the appropriate measure* and should be considered chaotic, whereas integrable Hamiltonians will not satisfy the constraints uniformly, in a

sense to be made more precise later.

6.1 Constrains from the Thermodynamic Limit

Let $H = \sum_{\langle i,j \rangle \in \mathcal{G}} h^{ij}$ be a Hamiltonian consisting of equivalent bi-local interaction terms $h^{ij} = h$ that act on pairs of n -elementary qudit subsystems, S_d , corresponding to neighboring vertices on an r -regular graph \mathcal{G} . A graph is r -regular if each vertex has r edges, resulting in $n_p = \frac{nr}{2}$ pairs of vertices connected by edges. The Hamiltonian acts on the Hilbert space $\mathcal{H} = \otimes^n \mathcal{H}_d$ which is the tensor product of the local Hilbert spaces \mathcal{H}_d associated to each elementary subsystem. The dimension \mathcal{H} is $N = d^n$, where d is the dimension of \mathcal{H}_d .

6.1.1 Density of states

The first property of H we wish to consider is the density of states in the thermodynamic limit. Let $\{E_\alpha\}$ be the spectrum of H and let $s_n(E) = \frac{1}{N} \sum_{\alpha=1}^N \delta(E - E_\alpha)$ be the corresponding density of states, normalized to be a probability distribution.

Theorem. As $n \rightarrow \infty$, the density of states $s_n(E)$ converges weakly to a Gaussian distribution with variance $\sigma_n^2 = \frac{n_p \text{tr}(h^2)^2}{2}$. By weak convergence it is meant that for any interval $[E/\sigma_n, E/\sigma_n + \epsilon/\sigma_n]$, the integral $N(E, \epsilon) \equiv \int_E^{E+\epsilon} s_n(E)$ converges to a Gaussian,

$$\lim_{\epsilon \rightarrow 0} \lim_{n \rightarrow \infty} N(E/\sigma_n, \epsilon/\sigma_n) = \frac{\epsilon/\sigma_n}{\sqrt{2\pi}\sigma_n} e^{-\frac{E^2}{2\sigma_n^2}}. \quad (6.1)$$

Proof I will proceed by showing that as $n \rightarrow \infty$ each moment m_k of $s_n(E)$ converges to the corresponding moment of a Gaussian distribution. Each moment is given by the trace of the corresponding power of the Hamiltonian, that is,

$$m_k \equiv \int E^k s_n(E) dE = \sum_{\alpha=1}^N E_\alpha^k = \frac{1}{N} \text{tr}(H^k).$$

The trace of H^k may be evaluated by expanding H^k in products of the bi-local terms h^{ij} and taking the trace of each product. Let ν_i indicate an edge in \mathcal{G} and let $\vec{\nu}$ be a k -length string of edges. Since each term, h^{ij} , in H corresponds to an edge in \mathcal{G} , it follows that $\text{tr}(H^k) = \sum_{\vec{\nu}} \text{tr}(h^{\nu_1} \dots h^{\nu_k})$,

where the sum is over all k -length strings of the n_p edges in \mathcal{G} . Each string, $\vec{\nu}$, may be partitioned into substrings $(\nu_{i_1} \dots \nu_{i_l}), \dots, (\nu_{j_1} \dots \nu_{j_p})$ such that the edges in each substring form disjoint connected subgraphs of \mathcal{G} . Since operators acting on different subsystems are algebraically independent, the trace of the operators labeled by a string factorizes into a product of traces of the operators labeled by the substrings, thus

$$\mathrm{tr}(h^{\nu_1} \dots h^{\nu_k}) = \mathrm{tr}(h^{\nu_{i_1}} \dots h^{\nu_{i_l}}) \dots \mathrm{tr}(h^{\nu_{j_1}} \dots h^{\nu_{j_p}}).$$

There may be many distinct strings $\vec{\nu}$ which can be partitioned into the same sets of equivalent substrings. Two substrings are taken to be equivalent if there is a graph translation that maps one substring to another.

Let the even and odd moments be considered separately. For even k , the partitioning that results from the largest number of distinct strings consists of $k/2$ substrings each containing exactly two copies of the same edge, with no two edges in different substrings sharing a vertex. For sufficiently large n_p , the number of sets of $k/2$ non-overlapping edges can be expressed as a polynomial in n_p whose leading order term is $\frac{n_p^{k/2}}{k/2}$. Since each edge occurs exactly twice in each string, there are $\frac{k!}{2^{k/2}}$ distinct strings for each such set of edges. The trace for the product of terms labeled by each such string is $N \left(\frac{\mathrm{tr}(h^2)}{2} \right)^{k/2}$. This yields a total contribution to $\mathrm{tr}(H^k)$ from this partitioning of

$$N \left(\frac{n_p \mathrm{tr}(h^2)}{2} \right)^{k/2} \frac{k!}{2^{k/2} (k/2)!} + \mathcal{O}(n_p^{k/2-1}).$$

Since all other partitionings of k -length strings are of lower order in n_p , and since the number of distinct partitionings is fixed for sufficiently large n_p , the above contribution dominates as $n \rightarrow \infty$. For odd k , the partitioning with the largest leading order in n_p consists of $\frac{k-3}{2}$ substrings containing exactly two copies of the same edge and one substring containing three edges. To leading order in n_p , there are $n_p^{k/2-1}$ strings that result in this partitioning.

Thus, the k th moment, m_k , of the density of states, $s_n(E)$, is given by

$$m_k = \frac{1}{N} \mathrm{tr}(H^k) = \begin{cases} \sigma_n^k \frac{k!}{2^{k/2} (k/2)!} + \mathcal{O}(n_p^{k/2-1}), & k \quad \text{even} \\ 0 + \mathcal{O}(n_p^{(k-3)/2}), & k \quad \text{odd} \end{cases}$$

where $\sigma_n^2 = \frac{n_p \text{tr}(h^2)}{2}$. To leading order in n these are precisely the moments of a Gaussian distribution with standard deviation σ_n . This is sufficient to prove weak convergence ■.

6.1.2 Microcanonical expectation values

Let A be an observable local to a subsystem S consisting of a *fixed* number m of elementary subsystems in the thermodynamic limit. Let the function $A_n(\{E_\alpha\}) \equiv \langle \alpha | A | \alpha \rangle$ map the spectrum $\{E_\alpha\}$ to the diagonal matrix elements with respect to the corresponding eigenstates $\{|\alpha\rangle\}$ of H . In the following, I provide a method for determining the smoothed function $A(E)$ to which $A_n(\{E_\alpha\})$ converges weakly in the thermodynamic limit. That is, I determine

$$\lim_{\epsilon \rightarrow 0} \lim_{n \rightarrow \infty} \sum_{\tilde{E} < E_\alpha / \sigma_n^2 < \tilde{E} + \epsilon} \langle \alpha | A | \alpha \rangle = A(\tilde{E}), \quad (6.2)$$

where $\tilde{E} \equiv E / \sigma_n^2 \sim E / n$ is a rescaled intensive energy variable proportional to the average energy per subsystem. The goal is to construct a power series expansion,

$$A(\tilde{E}) = \sum_{k=0}^{\infty} d_k \tilde{E}^k, \quad (6.3)$$

in terms of \tilde{E} . The method proceeds by constructing a $1/n$ expansion for each d_k ,

$$d_k = \sum_{p=0}^{\infty} \frac{d_{k,p}}{n^p},$$

and by retaining only the leading order term in the thermodynamic limit.

H is assumed at this point to be non-degenerate so that the set of powers H^k for $k = 0$ to $N - 1$ are linearly independent, and span the associative algebra of linear operators that commute with H , denoted here \mathcal{H}_C . Let

$$A_D \equiv \sum_{\alpha=1}^N \langle \alpha | A | \alpha \rangle | \alpha \rangle \langle \alpha |$$

be the projection of A onto \mathcal{H}_C . It follows that one may expand

$$A_D = \sum_{k=0}^{N-1} d_k \tilde{H}^k, \quad (6.4)$$

where $\tilde{H} = H/\sigma_n^2$. If for each k , d_k converges as $n \rightarrow \infty$, then it follows that $A_n(\{\tilde{E}_\alpha\})$ converges weakly to $A(\tilde{E})$ in the thermodynamic limit. In order to determine the coefficients, $\{d_k\}$, an orthonormal basis of operators spanning \mathcal{H}_C is required. Such a basis may be obtained by starting with the linearly independent set, $(H^0, H \dots, H^{N-1})$, and performing Gram-Schmidt orthogonalization to obtain a new set of operators, $\{G_k\}$, such that $\text{tr}(G_k G_{k'}) = \delta_{kk'}$. The resulting operators may be expressed in terms of the moments, m_k , of H^k as the following Vandermonde determinant:

$$G_k = \det \begin{pmatrix} m_0 & m_1 & \cdots & m_k \\ m_1 & m_2 & \cdots & m_{k+1} \\ \vdots & \vdots & \vdots & \vdots \\ 1 & H & \cdots & H^k \end{pmatrix}.$$

It follows that $\text{tr}(H^{k'} G_k) = 0$ if $k' < k$ since two of the rows in the determinant will then be the same. Since $G_{k'}$ has components only along H^0 to $H^{k'}$ it follows that $\text{tr}(G_k G_{k'}) = 0$ if $k \neq k'$. The operators G_k may be considered orthogonal polynomials in the continuous parameter E with respect to the density of states, $s_n(E)$, that is,

$$\text{tr}(G_k G_{k'}) = \int dE G_k(E) G_{k'}(E) s_n(E) = \delta_{kk'}.$$

In terms of the G_k , A_D may now be expanded as

$$A_D = \sum_{k=0}^{N-1} c_k G_k, \quad (6.5)$$

where $c_k = \text{tr}(G_k A)$. The goal now is to obtain the coefficients $\{d_k\}$ entering Eq.(6.3) in terms of the $\{c_k\}$.

We begin with an examination of the coefficients $c_k = \text{tr}(G_k A)$ for an observable A local to a subsystem S , as $n \rightarrow \infty$. The first thing to note is that since, since $s_n(E)$ converges to a Gaussian

with variance $\sim \sqrt{n_p}$, as $n \rightarrow \infty$, each polynomial $\{G_k\}$ converges to the corresponding Hermite polynomial. That is, each G_k may be expressed, $G_k = \sum_{l=0}^k (a_l^k + \mathcal{O}(n_p)^{-1}) \frac{E}{(\sqrt{n_p})^{k/2}}$ where $\{a_l^k\}$ are the exact coefficients describing Hermite polynomials. The goal now is to show that to leading order in n_p , $c_k = c_k^1/n_p^{k/2} + \mathcal{O}(n_p^{k/2-1})$. Then when substituted into Eq. 6.5, the only term that does not go to zero as $n \rightarrow \infty$ with $\tilde{E} \sim E/n_p$ held fixed is highest order term (of power E^k) in each G_k . And from the combinatorial and normalization properties of Hermite polynomials it follows that,

$$A_D = \sum_{k=1}^{\infty} \frac{c_k^1}{k!} \tilde{E}^k. \quad (6.6)$$

The method of expanding smoothed expectation values for non-integrable many-body systems in terms of such orthogonal polynomials was developed by French and co-authors in [9, 71, 72]. This method has been applied extensively to nuclear shell model calculations for strength functions (off-diagonal variances here), and to ensemble averages of embedded random matrix ensembles (EGOE), which consist of randomly selected two-body interactions between fermions. To our knowledge, however, this method has not been applied to determining the thermodynamic limit for a Hamiltonian with a fixed lattice and interaction form.

6.1.3 Correlation functions

Next, I will show how weak constraints on correlations between off-diagonal matrix elements of local observables can be constructed analogous to those for the diagonal matrix elements by means of an appropriate expansion of dynamical correlation functions between arbitrary local observables in frequency space. The method begins by expanding $A_t \equiv e^{iHt} A e^{-iHt}$ using the Baker-Hausdorff Lemma,

$$A_t = \sum_{l=0}^{\infty} \frac{(it)^l}{l!} [H, A]_l, \quad [A, B]_l \equiv [A, [A, [\dots [A, B] \dots]]].$$

Now let $A_\omega = \int_0^\infty A_t e^{-i\omega t} dt$. Then, it follows that,

$$\frac{d^l}{dt^l} A_t = \int_{-\infty}^{\infty} (-i\omega)^l A_\omega e^{-i\omega t} d\omega.$$

In conjunction with Eq.(6.7) this yields,

$$[H, A]_l = \left[\frac{d^l}{dt^l} A_t \right]_{t=0} = \int_{-\infty}^{\infty} \omega^l A_\omega d\omega.$$

For two observables A and B local to a subsystem S , let the correlation function at energy \tilde{E} be defined as

$$C_{AB}(\tilde{E}, \epsilon, t) \equiv \frac{1}{N(\tilde{E}, \epsilon)} \text{tr}(\Pi(\tilde{E}, \epsilon) B A_t),$$

where $\Pi(\tilde{E}, \epsilon)$ is the projector onto the subspace $W(\tilde{E}, \epsilon)$ spanned by energy eigenstates, $|\alpha\rangle$, such that $\tilde{E} < E_\alpha/\sigma_n^2 < \tilde{E} + \epsilon$. By a generalization of the Wiener-Khinchin theorem [74] to cross-correlations, the corresponding power spectrum is given by the Fourier transform of the correlation function,

$$\tilde{C}_{AB}(\tilde{E}, \epsilon, \omega) = \int_0^\infty C_{AB}(\tilde{E}, t, \epsilon) e^{i\omega t} dt = \frac{1}{N(\tilde{E}, \epsilon)} \text{tr}(\Pi(\tilde{E}, \epsilon) B A_\omega). \quad (6.7)$$

Thus, the l -th moment $\Omega_{AB}^l(\tilde{E}, \epsilon)$ of $\tilde{C}_{AB}(\tilde{E}, \epsilon, \omega)$ is given by

$$\Omega_{AB}^l(\tilde{E}, \epsilon) \equiv \int_{-\infty}^{\infty} \omega^l \tilde{C}_{AB}(\tilde{E}, \epsilon, \omega) d\omega = \frac{1}{N(\tilde{E}, \epsilon)} \text{tr}(\Pi(\tilde{E}, \epsilon) B [H, A]_l). \quad (6.8)$$

Since $B[H, A]_l$ is a local operator, its projection onto the commutant \mathcal{H}_C may be expanded in the thermodynamic limit as

$$B[H, A]_l = \sum_{k=1}^{\infty} c_k^l G_k.$$

In conjunction with Eq. (6.8), this results in the following expansion for each moment:

$$\Omega_{AB}^l(\tilde{E}) = \sum_k \frac{d_k^l}{k!} \tilde{E}^k. \quad (6.9)$$

The set of all moments $\Omega_{AB}^l(\tilde{E})$ are a weak constraint on the function $\tilde{C}_{AB}(\tilde{E}, \epsilon, \omega)$.

The set of all spectral correlation functions $C_{AB}(\tilde{E}, \epsilon, t)$ for operators local to a subsystem S is equivalent to the evolution operator $\Lambda_S(\rho, t) = \text{tr}_S(U_t \rho U_t^\dagger)$ reduced to S . Thus, the weak constraints on the set $\{\tilde{C}_{AB}(\tilde{E}, \epsilon, \omega)\}$ in the thermodynamic limit induce a smoothing on $\Lambda_S(\rho, \omega) = \int_0^\infty dt \Lambda_S(\rho, t) e^{-i\omega t}$. Consider the family $\{\Lambda_{S_i}(\rho, \omega)\}$ of smoothed propagators for a sequence of sub-

systems S_i such that $S_i \subset S_{i+1}$. Then, if there exists a set of eigenvalues of Λ_{S_i} and corresponding eigenvectors that converge as $i \rightarrow \infty$, this defines a quantum many-body Frobenius-Perron operator with each eigenvalue labeling a ‘‘Ruelle-Pollicott’’ resonance, as introduced in [75] for many-body systems without a classical analogue. The gap Δ between the largest such eigenvalue with magnitude less than 1 and the unit eigenvalue corresponding to the equilibrium density matrix yields the asymptotic (long-time) relaxation rate of the system to equilibrium. The corresponding relaxation time, referred to as the Thouless time [76], is given by $t_{Th} = \frac{1}{\ln(1-\Delta)}$.

The constraints on the correlation functions may also be expressed in terms of empirical covariances of the corresponding matrix elements. Since the following relations hold,

$$C_{AB}(\tilde{E}, \epsilon, t) = \frac{1}{N(\tilde{E}, \epsilon)} \sum_{E_\alpha \in W(\tilde{E}, \epsilon), E_\beta} \langle \alpha | A | \beta \rangle \langle \beta | B | \alpha \rangle e^{-i(E_\alpha - E_\beta)t}, \quad (6.10)$$

$$\tilde{C}_{AB}(\tilde{E}, \epsilon, \omega) = \lim_{\delta\omega \rightarrow 0} \lim_{n \rightarrow \infty} \frac{1}{N(\tilde{E}, \epsilon)} \sum_{\substack{E_\alpha \in W(\tilde{E}, \epsilon) \\ \omega < E_\alpha - E_\beta < \omega + \delta\omega}} \langle \alpha | A | \beta \rangle \langle \beta | B | \alpha \rangle, \quad (6.11)$$

this implies a weak constraint on the empirical covariance above for matrix elements of A and B in the eigenbasis of H . It is useful to analyze the constraints on the auto-correlation function (where $A = B$) through an empirical variance, $v_n(E, \epsilon, \omega, \delta\omega)$, defined as follows (cf Eq.5.5):

$$v_n(E, \epsilon, \omega, \delta\omega) \equiv \left[\frac{1}{N(E, \epsilon)N(E + \omega, \delta\omega)} \sum_{\substack{E < E_\alpha < E + \epsilon \\ \omega < E_\alpha - E_\beta < \omega + \delta\omega}} |\langle \alpha | A | \beta \rangle - \delta_{\alpha\beta} A(E)|^2 \right]. \quad (6.12)$$

The sum of the squared moduli of the off-diagonal matrix elements between an energy eigenstate $|\alpha\rangle$ and all other energy eigenstates is given by the corresponding diagonal matrix element of A^2 ,

$$(A^2)_{\alpha\alpha} = A_{\alpha\alpha}^2 + \sum_{\beta \neq \alpha} |A_{\alpha\beta}|^2.$$

Since A is local to a fixed subsystem S , the energy width over which the off-diagonal matrix elements are non-zero is constant in the thermodynamic limit, reflecting the fact that a local observable may

only alter the energy contribution from the projection of H onto S . Since in the thermodynamic limit, $A(\tilde{E})$ and $A^2(\tilde{E})$ converge with respect to $\tilde{E} \sim E/n$, it follows that if the empirical variance converges, then it is given by a representation of the delta function $nf(\tilde{E}, (\tilde{E}' - \tilde{E})n)$ along the diagonal, that is,

$$v_n(\tilde{E}, \omega) \rightarrow \frac{nf(\tilde{E}, \omega)}{s(\tilde{E} + \omega/\sigma_n^2)} [A^2(\tilde{E}) - A(\tilde{E})^2]. \quad (6.13)$$

where $\omega = E - E'$. If the decay of the autocorrelation function $C_{AA}(\tilde{E}, t) \sim e^{-\Gamma t}$ is exponential, the corresponding envelope function $f(\tilde{E}, \omega)$ is characterized by a Lorentzian peak with linewidth Γ .

6.1.4 Concentration of measure and quantum ergodicity

As shown above, the thermodynamic limit imposes *weak* constraints on the eigenvectors and eigenvalues of arbitrary many-body Hamiltonians. That is, the constraints are required to hold only for averages over finite energy windows. Remarkably, these constraints do not depend on whether H is integrable, rather we will argue that the way in which the constraints are satisfied distinguishes whether the system is integrable, partially integrable, or fully chaotic. There are three possibilities for how the constraints on the diagonal matrix elements may be satisfied.

6.1.4.1 Weak convergence only

For an example where only weak convergence occurs, consider the Ising Hamiltonian, $H = \sum_{\langle i, j \rangle \in \mathcal{G}} \sigma_z^i \sigma_z^j$ for nearest neighbors on a regular lattice \mathcal{G} . This Hamiltonian is trivially integrable since each of the interaction terms commute. The eigenbasis is given by the computational basis. The expectation values for any interaction term with respect to the energy eigenstates can take on only two values, $\langle \alpha | \sigma_z^i \sigma_z^j | \alpha \rangle = \pm 1$, yet the weak constraint is given by $\sigma_z^i \sigma_z^j(\tilde{E}) = \tilde{E}$. Thus, it is obvious that the diagonal matrix elements only converge in a weak sense.

6.1.4.2 Strong convergence only

The convergence will be said to be strong, if for all local observables, A , and all ϵ' there exists a $\delta\omega$ such that

$$\lim_{n \rightarrow \infty} \sup \frac{1}{N(\tilde{E}, \epsilon)} \sum_{\substack{E_\alpha, E_\beta \in W(\tilde{E}, \epsilon) \\ |E_\alpha - E_\beta - \omega| < \delta\omega}} |\langle \alpha | A | \beta \rangle|^2 < \epsilon'. \quad (6.14)$$

That is, the diagonal and off-diagonal matrix elements converge strongly if the fluctuations around the mean of zero for off-diagonal matrix elements and $A(\tilde{E})$ for diagonal matrix elements vanish in the thermodynamic limit. Strong convergence has the important consequence of weak dynamical mixing [56]. That is, since the diagonal matrix elements converge strongly in the thermodynamic limit, then for any initial state the time average is given by the microcanonical average $A(\tilde{E})$ [46], and since the off-diagonal matrix elements go to zero, the fluctuations around the microcanonical value must also, vanish. It is important to note that a system may be integrable yet still have strongly converging matrix elements, though as shown in Ch.7 for integrable systems the convergence tends to be slow and the fluctuations may be specific to the system Hamiltonian.

6.1.4.3 Strong convergence with universal fluctuations

The strongest form of convergence for matrix elements in the thermodynamic limit is given by universal scaling laws that are related to random matrix ensembles. This case may be summarized by the statement that the eigenvectors are as random as possible subject to all prior constraints. This intuition, applied in [61, 63, 77], underlies the application of random matrix theory to quantum chaos. If the matrix elements are uniformly distributed subject to the constraints on their mean and variance, then the empirical distribution will be approximately Gaussian in the thermodynamic limit. The probability that any matrix element is much larger than the corresponding variance falls exponentially. Thus almost every matrix element deviates from its mean value by no more than $1/s_n(\tilde{E}) \sim 1/2^n$ for many body systems. This is a manifestation of the phenomenon of *concentration of measure*, whereby for vectors selected uniformly with respect to the Haar measure from a large dimensional Hilbert space, the fluctuations from the mean can be tightly bounded for well-behaved functions [78, 79]. When a Hamiltonian satisfies the thermodynamic constraints

uniformly at random, well-behaved functionals of the eigenstates are satisfied with high probability due to concentration of measure. Thus, even though arbitrary eigenstates of a many-body quantum system are intractably complicated, requiring an exponentially growing number of parameters in n in order to specify, all of the stable information about the structure of the eigenstates is contained in either the thermodynamic constraints, which in the neighborhood of $\tilde{E} = 0$ are analytically tractable, or in the fluctuations around those constraints, which if uniform become highly predictable the larger the dimension of the system Hilbert space. In the following chapter, a numerical example will be used to demonstrate the above conjectures and results.

Chapter 7

XX Model on Random Graphs

7.1 Model Hamiltonian

In this chapter a simple model many-body Hamiltonian is investigated numerically to illustrate the analytical results and conjectures presented in Ch.6. The model system consists of nearest neighbor interactions between n two-state subsystems (qubits) each located at the vertex of an n -vertex graph \mathcal{G} . Let $H = \sum_{\langle i,j \rangle \in \mathcal{G}} h^{ij}$, where $h^{ij} = \sigma_x^i \sigma_x^j + \sigma_y^i \sigma_y^j$ is the so-called hopping (or flip-flop) operator, and let \mathcal{G} be a 3-regular random graph. A natural basis for the n -qubit Hilbert space \mathcal{H} is given by the joint eigenstates of a complete set of independent local operators $\{\sigma_z^i\}$. This basis can be labeled by strings of 1's and 0's, indicating the eigenvalue for each σ_z^i operator by, $\sigma_z^i|0\rangle = |0\rangle$ and $\sigma_z^i|1\rangle = -|1\rangle$ and will be referred to as the *computational* basis. In the computational basis, the hopping operator acts as follows:

$$h|01\rangle = |10\rangle, \quad h|10\rangle = |01\rangle, \quad h|00\rangle = 0, \quad h|11\rangle = 0. \quad (7.1)$$

The 3-regular random graph \mathcal{G} is constructed by selecting edges uniformly at random until each vertex has exactly 3 edges, yielding $3n/2$ edges total. Because 3 is odd, 3-regular graphs can only be constructed for even numbers of vertices. An example of a 3-regular random graph for $n = 14$ qubits is shown in Fig. 7.1.

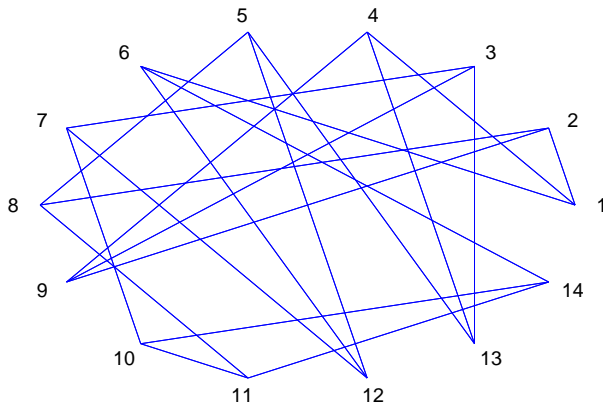


Figure 7.1: Schematic representation of a 3-regular random graph for $n = 14$.

7.1.1 Symmetries

Since the action of the hopping term h does not change the number of 1's and 0's in a computational basis state, it follows that H commutes with the operator $S_z = \sum_i^n \sigma_z^i$. Additionally, H is invariant under the discrete symmetry, $\sigma_x^{\otimes n}$, which maps $|0\rangle \rightarrow |1\rangle$ and $|1\rangle \rightarrow |0\rangle$ for each qubit. However, since this mapping connects states belonging to different S_z eigenspaces, it does not introduce new invariant subspaces, except in the central subspace labeled by $S_z = 0$ when n is even. One may project the Hamiltonian into each invariant subspace of S_z , and construct weak constraints for the density of states and matrix elements for each projection. Although the average over all of the weak constraints for each of the projected Hamiltonians is equivalent to the weak constraints on the full Hamiltonian, the constraints for any particular subspace may differ substantially. However, for subspaces that are asymptotically half full, that is, $S_z/n \rightarrow 0$ as $n \rightarrow \infty$, the subspace constraints do not differ from the constraints for the full Hamiltonian in the thermodynamic limit, since half filling is indistinguishable from having no constraint on the number of 1's or 0's for any fixed subsystem S in the thermodynamic limit.

Because the lattice is random, H is not invariant under any symmetries arising from lattice geometry, whereas for example a Bravais lattice can be invariant under multiple independent lattice

transformations which define crystal momentum under closed boundary conditions and parity under open boundary conditions. A randomly generated lattice is unlikely to possess any such symmetries. Since in the standard basis described, the matrix elements of H are real, it follows that H belongs to the GOE universality class, since this basis can be defined without reference to the detailed structure of the eigenvectors of H . The subspace with $S_z = 1$ will be chosen for detailed examination in what follows.

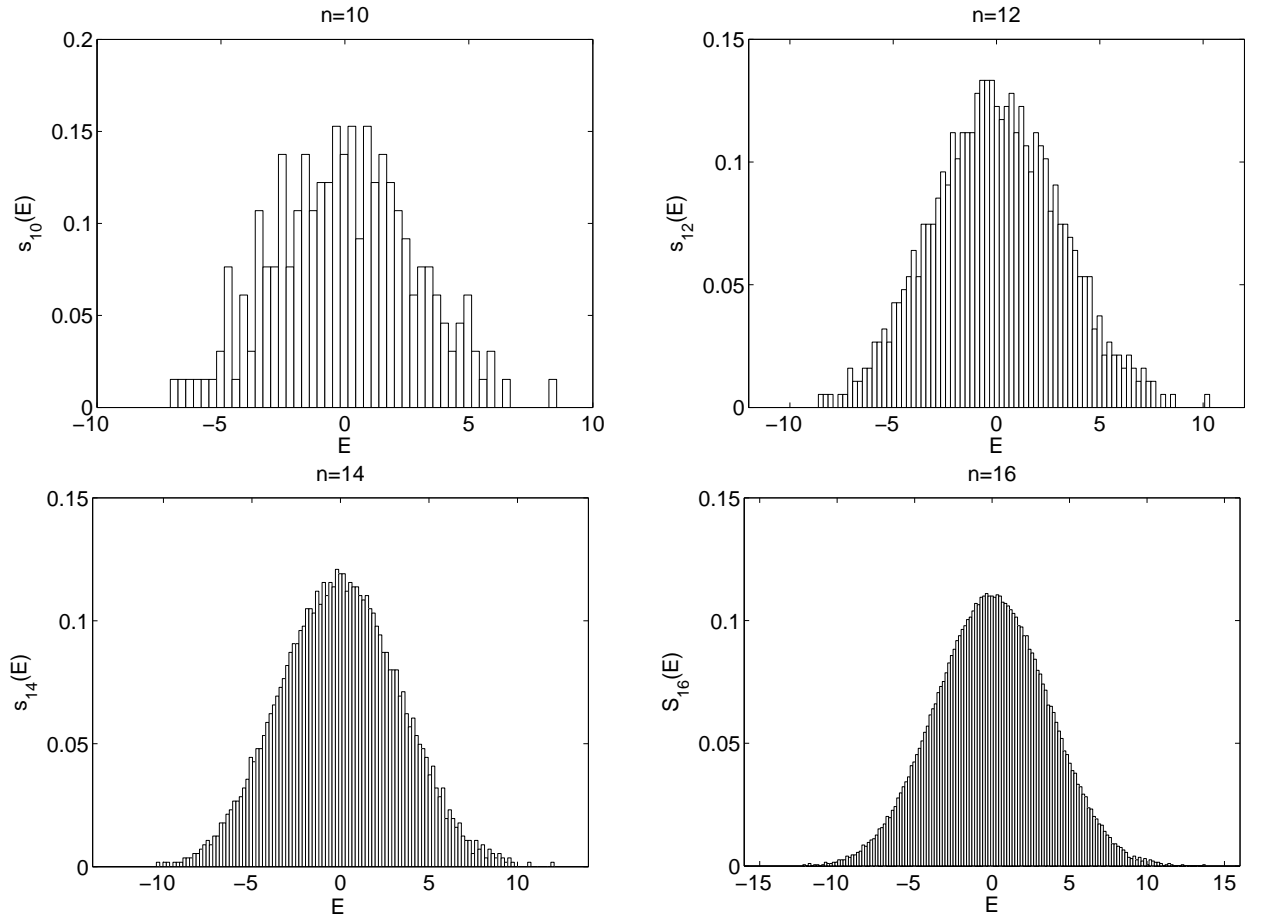


Figure 7.2: Smoothed density of states $s_n(E)$ for $n = 10, 12, 14, 16$ for the subspace with $S_z = 1$.

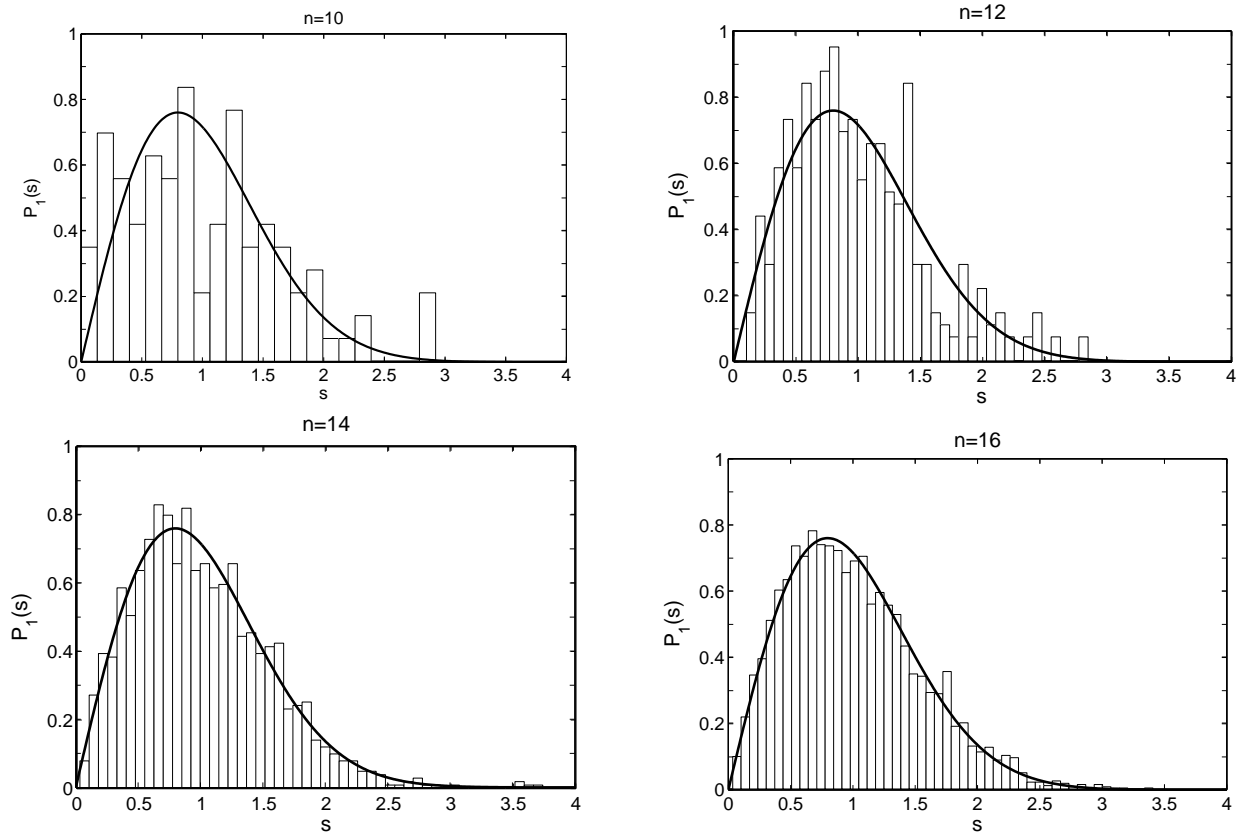


Figure 7.3: Empirical energy level spacing distribution $P_1(s)\delta s$ for the interval $-2 < E_\alpha < 2$ for $n = 10$ (top left), $n = 12$ (top right), $n = 14$ (bottom left) and $n = 16$ (bottom right).

7.2 Eigenvalue Properties

In Fig. 7.2 the density of states $s_n(E) = \frac{1}{N} \sum_{\alpha=1}^N \delta(E - E_\alpha)$ for $n = 10, 12, 14, 16$ has been smoothed by counting how many eigenvalues fall into a set of intervals. Significant convergence to the predicted Gaussian is apparent for this range of n . In Fig.7.3 the nearest neighbor level spacing distribution, $P_1(s)ds$, is shown for the eigenvalues in an interval $-2 < E_\alpha < 2$. Convergence to the Wigner-Dyson distribution, $P_1(s)ds = \frac{\pi s}{2} e^{-\frac{\pi s^2}{4}}$ is equally fast. However, for segments of the energy spectrum that are far from the center, $P_1(s)ds$ deviates increasingly from random matrix theory, becoming approximately Poissonian at the extremes. It is an interesting question whether in the thermodynamic limit the border between chaos in the energy spectrum is sharp or soft.

7.3 Eigenvector Properties

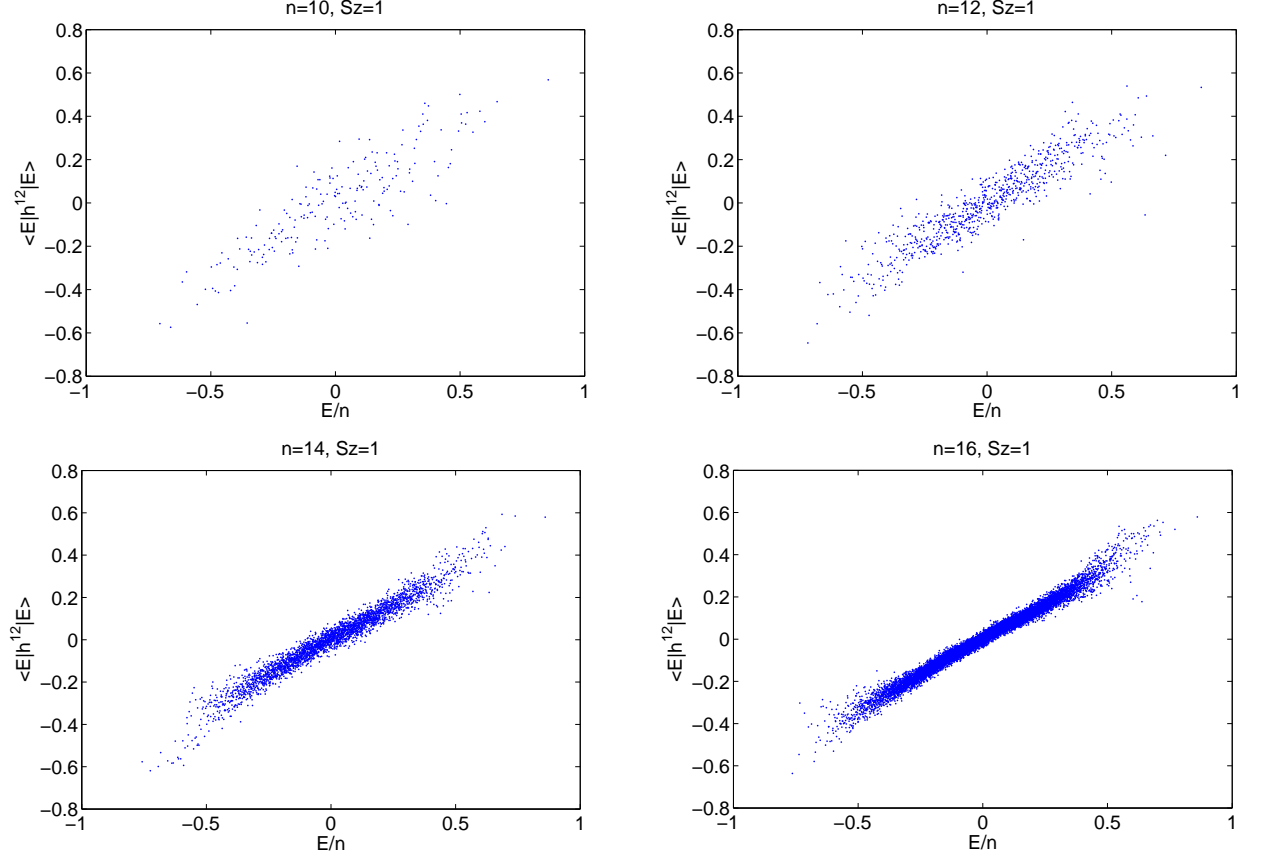


Figure 7.4: Diagonal matrix elements $\langle \alpha | h^{12} | \alpha \rangle$ for the interaction term between neighboring vertices 1 and 2 in \mathcal{G} as a function of rescaled energy eigenvalues $\{E_\alpha/n\}$ with for $n = 10, 12, 14$, and 16.

Consider the interaction term h^{12} between the neighboring vertices 1 and 2 in \mathcal{G} . Since a regular random graph is homogenous in the thermodynamic limit, in the sense of no point in the lattice being favored over another, and since $\sum_{\langle i,j \rangle \in \mathcal{G}} \langle \alpha | h^{ij} | \alpha \rangle = E_\alpha$, it follows that in the thermodynamic limit the expression for $\overline{\langle \alpha | h^{12} | \alpha \rangle} \equiv h^{12}(\tilde{E})$ is given by $h^{12}(\tilde{E}) = \frac{E}{\sigma_n^2} = \tilde{E}$. The diagonal matrix elements $\langle \alpha | h^{12} | \alpha \rangle$ are plotted in Fig. 7.4 for $n = 10, 12, 14, 16$. Note that concentration around the thermodynamic constraint occurs for relatively small size system.

To quantify the rate at which concentration of the matrix element occurs, the fluctuations are averaged from $-2 < E_\alpha < 2$ for each n , in which region the diagonal variance, $v_D(\tilde{E})$, remains

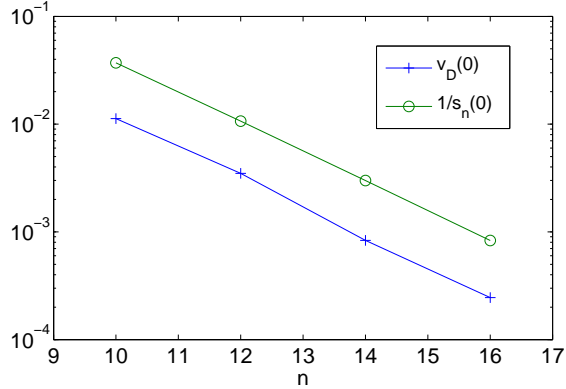


Figure 7.5: Diagonal variance $v_D(0)$ at $\tilde{E} = 0$ for an interaction term h^{12} where 1 and 2 are neighboring vertices in \mathcal{G} as a function of n . The inverse density of states $1/s_n(0)$ evaluated at $\tilde{E} = 0$ is also given for comparison.

approximately constant with \tilde{E} . The scaling of the fluctuations with respect to n around the smoothed energy dependence is shown in Fig. 7.3. Note that the empirical variance of diagonal matrix elements scales inversely with the density of states, $s_n(\tilde{E})$, in agreement with the case of strong convergence with universal fluctuations described in Ch. 6.

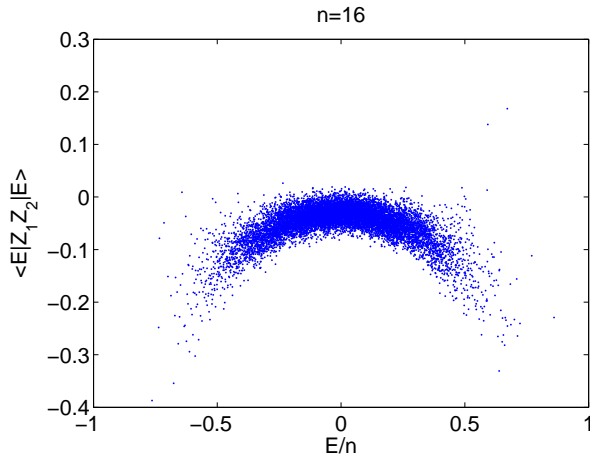


Figure 7.6: Diagonal matrix elements $\langle \alpha | \sigma_z^1 \sigma_z^2 | \alpha \rangle$ where 1 and 2 are neighboring vertices in \mathcal{G} as a function of rescaled energy eigenvalues $\{E_\alpha/n\}$ with $n = 16$.

Next we consider are expectation values of a correlation term $\langle \alpha | \sigma_z^1 \sigma_z^2 | \alpha \rangle$ between two neighboring vertices on \mathcal{G} . Since $\text{tr}(H \sigma_z^1 \sigma_z^2) = 0$, but $\text{tr}(H^2 \sigma_z^1 \sigma_z^2) \neq 0$ for sufficiently small \tilde{E} and large n , $\sigma_z^1 \sigma_z^2(\tilde{E}) \sim \tilde{E}^2$. The quadratic behavior is accurately predicted by the coefficient in the thermody-

dynamic limit as shown in Fig. 7.6.

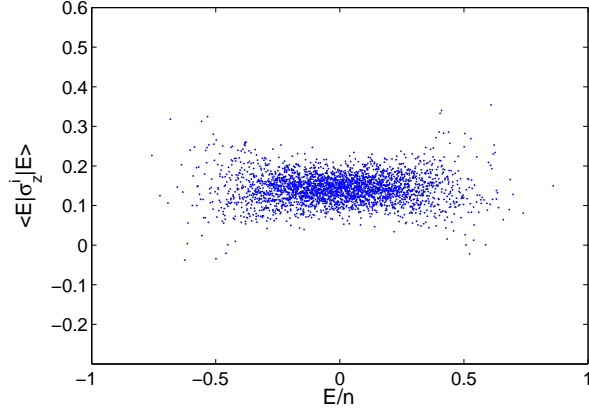


Figure 7.7: Diagonal matrix elements $\langle \alpha | \sigma_z^1 | \alpha \rangle$ of a single-qubit σ_z operator on vertex 1 of \mathcal{G} as a function of rescaled energy eigenvalues $\{E_\alpha/n\}$ with $n = 14$.

For sufficiently large n , $\text{tr}(H^k \sigma_z^i) = 0 \forall k$. Thus, the thermodynamic expression is given by $\sigma_z^1(\tilde{E}) = 0$. One expects $\langle \alpha | \sigma_z^1 | \alpha \rangle$ to be dominated by random fluctuations, as can be seen in Fig. 7.7. Since $\sigma_z^2 = I$, it follows that $\sigma_z^2(\tilde{E}) = 1$, and thus the strength of the fluctuations as a function of \tilde{E} is determined solely by the density of states.

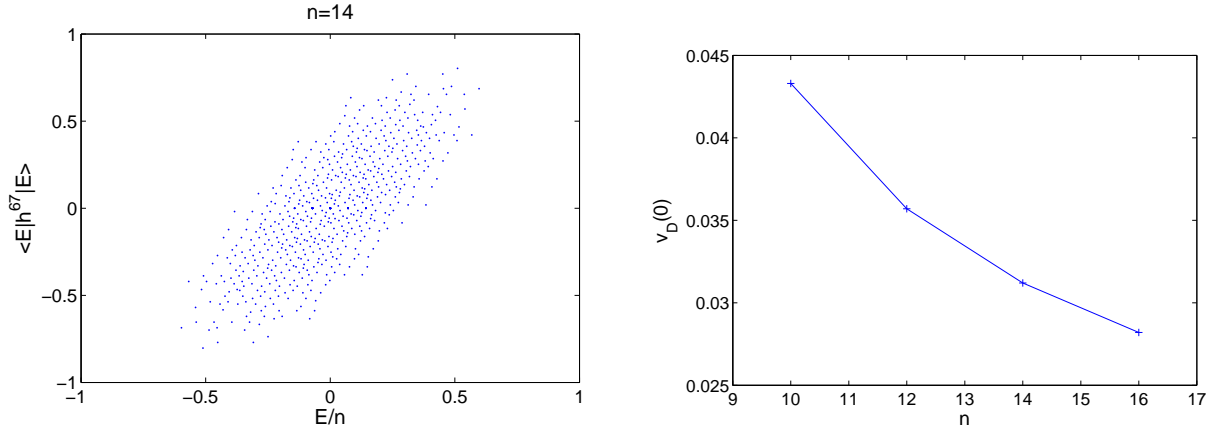


Figure 7.8: Left: Diagonal matrix elements for the interaction term h^{67} of the integrable 1D hopping Hamiltonian where $n = 14$, Right: Diagonal variance $v_D(0)$ for $E = 0$ for $n = 10, 12, 14, 18$.

For comparison the Hamiltonian $H = \sum_{i=1}^{n-1} h^{ii+1}$ is integrable by Jordan-Wigner transformation. The diagonal matrix elements for the interaction term h^{67} for $n = 14$ are shown in Fig. 7.8. Note

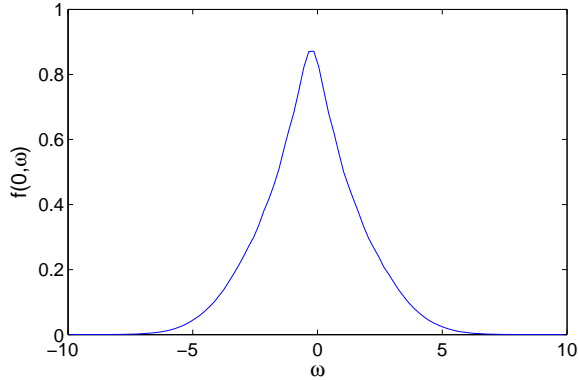


Figure 7.9: Envelope function $f(\tilde{E}, \omega)$ evaluated at $\tilde{E} = 0$ for the empirical variance of off-diagonal matrix elements $\langle \alpha | h^{12} | \beta \rangle$ of the interaction term h^{12} between a pair of neighboring vertices on \mathcal{G} with $n = 14$.

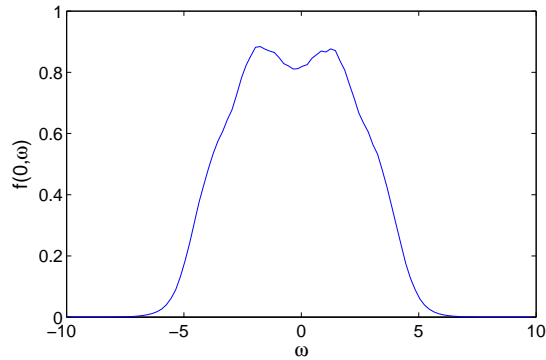


Figure 7.10: Envelope function $f(\tilde{E}, \omega)$ evaluated at $\tilde{E} = 0$ for the empirical variance of off-diagonal matrix elements $\langle \alpha | \sigma_z^1 | \beta \rangle$ single-qubit σ_z operator on site 1 with $n = 14$.

that compared to the non-integrable hopping Hamiltonian on a random graph the diagonal matrix elements are far less concentrated. As indicated in the right panel of Fig. 7.8 the diagonal variance decreases with n indicating strong convergence although the rate is slow.

The envelope function describing the empirical variance off-diagonal elements of σ_z^1 , and h^{12} are shown for $n = 14$ in Fig. 7.10 and Fig. 7.9 respectively. For h^{12} the shape of the envelope function is approximately Lorentzian, with a cut-off at the tails of the distribution. The envelope function for σ_z^1 has two approximate Lorentzian peaks each at an offset from $\tilde{E} - \tilde{E}' = 0$.

7.4 Entanglement of Chaotic Eigenstates

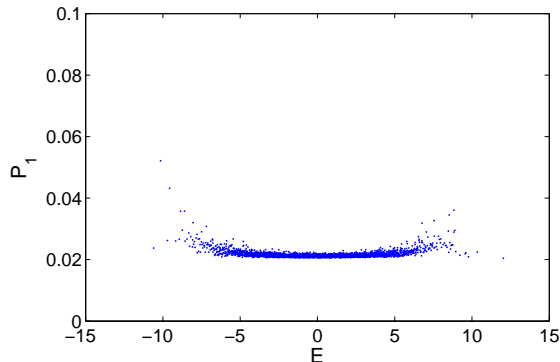


Figure 7.11: Local purity \mathcal{P}_1 of the eigenstates of H as a function of energy eigenvalue with $n=14$.

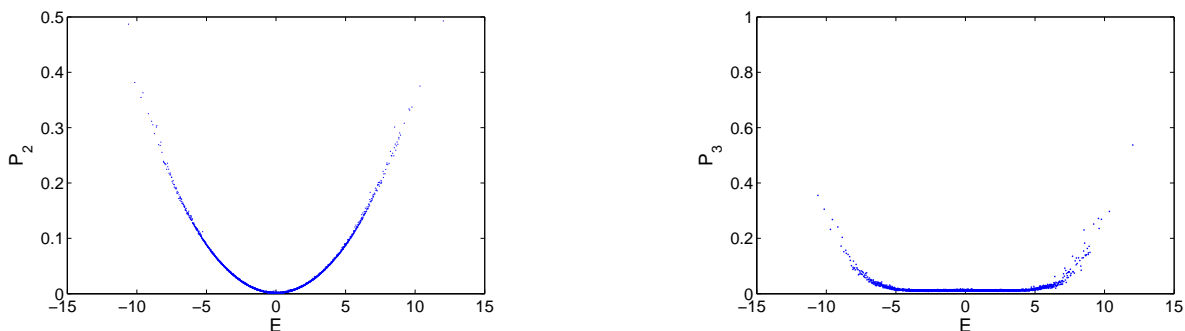


Figure 7.12: Bi-local \mathcal{P}_2 and 3-local \mathcal{P}_3 of the eigenstates of H as a function of energy eigenvalue with $n=14$.

We next examine the entanglement content of the eigenvectors of H . Entanglement is a purely quantum mechanical property and its role in quantum chaos and thermalization is an open area of investigation. Numerical results examining entanglement content of the eigenvectors of a many-body system with Heisenberg interactions across transitions from integrability to chaos are examined in [80, 81]. Here insight from orthogonal polynomial expansions for local observables will be employed to understand some general features of the entanglement of the eigenstates of chaotic Hamiltonians.

One simple approach to defining how entangled a quantum pure state is, is to ask how little information is available to *local* measurements, since entanglement should be understood as the information content of the state that is hidden on non-local correlations. Arguably, the simplest

entanglement measure for pure states of a many-body system is provided by the local purity [82, 83],

$$\mathcal{P}_1(|\psi\rangle) = \frac{1}{n} \sum_{i=1}^n \sum_{\alpha=x,y,x} \langle \psi | \sigma_\alpha^i | \psi \rangle^2.$$

This measure quantifies how much information is obtainable about the state $|\psi\rangle$ through knowledge of expectation values observables local to n single-qubit subsystems. Because H commutes with the z -component of the total spin S_z , it follows that, $\langle \alpha | \sigma_x^i | \alpha \rangle = \langle \alpha | \sigma_y^i | \alpha \rangle = 0$ for all i . However, $\langle \alpha | \sigma_z^i | \alpha \rangle$ is not required to be zero, but since $\text{tr}(G_k \sigma_z^i) = 0$ for all k polynomial in n , it follows that the smooth energy dependence on σ_z is a constant determined by the S_z subspace. Thus, the local purity depends only on the size of the fluctuations around the smoothly varying energy dependence of $\langle \alpha | \sigma_z^i | \alpha \rangle$.

One may define an entanglement measure that is sensitive to how much information can be obtained by a courser decomposition of the system into subsystems, in this case subsystems consisting of neighboring pairs of qubits on \mathcal{G} . I shall refer to this measure as bi-local purity, defined as follows,

$$\mathcal{P}_2(|\psi\rangle) = \frac{c_2}{n_p} \sum_{\langle i,j \rangle} \sum_{\alpha,\beta=x,y,z} \langle \psi | \sigma_\alpha^i \sigma_\beta^j | \psi \rangle^2.$$

where c_2 is a normalization constant to insure that the maximum possible value of \mathcal{P}_2 is 1. Since the bi-local purity contains the expectation values of the energy interaction terms, it shows a strong dependence on energy. The form of the dependence is quadratic to first order since $h^{ij}(E) = \frac{E}{n_p}$ is a linear dependence. One may continue in this way defining entanglement measures that probe information available to measurements on increasingly larger subsystems. Let the 3-local purity be defined as,

$$\mathcal{P}_3(|\psi\rangle) = \frac{c_3}{n_p} \sum_{\langle i,j,k \rangle} \sum_{\alpha,\beta,\gamma=x,y,z} \langle \psi | \sigma_\alpha^i \sigma_\beta^j \sigma_\gamma^k | \psi \rangle^2.$$

where $\langle i, j, k \rangle$ are sets of three consecutive vertices on \mathcal{G} . The lowest order in H for which $\text{tr}(H^k \sigma_\beta^j \sigma_\gamma^k) \neq 0$ is $k = 2$, which generates an interaction term h^{ik} and a density correlation $\sigma_z^i \sigma_z^k$ where vertices i and k are distance 2 away. Thus, to lowest order, \mathcal{P}_3 is given by a quartic polynomial in the thermodynamic limit. At the center of the spectrum, any traceless observable A , $A(0) = 0$,

and so the average purity and the corresponding entanglement is completely determined by the fluctuations around the smoothed microcanonical expectation value. If the fluctuations are universal, then the the average entanglement of such eigenstates will be equal to those of random states with respect to the Haar measure.

7.5 Dynamics

The time evolution for some initial states is calculated for expectation values of $\langle \psi_1 | h^{ij}(t) | \psi_1 \rangle$ and $\langle \psi_2 | \sigma_z^i(t) | \psi_2 \rangle$ for a pairs (i, j) of neighboring vertices with $n = 14$ for both a 3-regular random graph which is chaotic for energies near the center of the spectrum, and a 2-regular open chain, which is integrable via Jordan-Wigner transformation. The time evolution is plotted in Fig. time.

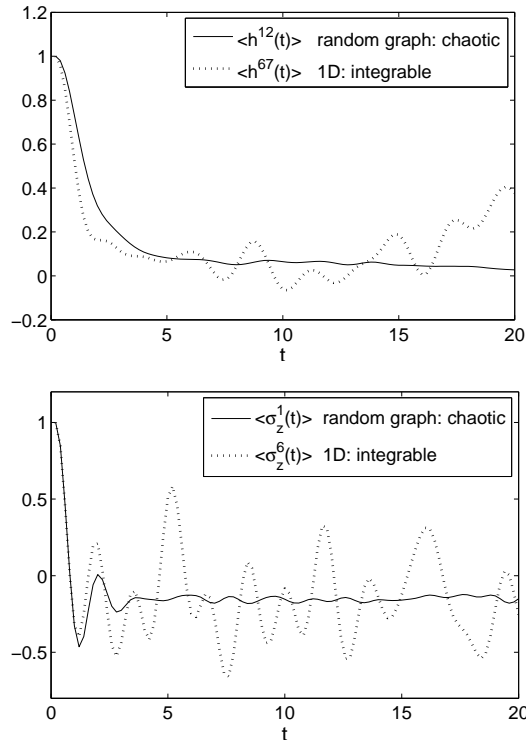


Figure 7.13: Top: Time evolution for an interaction term $\langle h(t) \rangle$ for a random 3-regular graph and an 1D open chain with $n = 14$. Bottom: Time evolution for $\langle \sigma_z(t) \rangle$.

Let $|\psi_1\rangle$ be a product of a Bell state $\frac{1}{\sqrt{2}}(|01\rangle + |10\rangle)$ with a computational basis state and let

$|\psi_2\rangle$ be a computational basis state.

For all cases there is an initial decay from a maximum value of the operator governed by the envelope function $f(\tilde{E}, \omega)$. For the σ_z operators there is an oscillation consistent with the double peaked form of $f(\tilde{E}, \omega)$. For the chaotic systems the decay reaches a pronounced steady state which is close to the microcanonical value. For h^{12} the predicted equilibrium value is $1/21=0.0476$, since for the initial state $\langle\psi_1|h^{12}|\psi_1\rangle = 1$ and $\langle\psi_1|h^{ij}|\psi_1\rangle = 0$ for all other neighboring vertices i and j . The average value of $\langle\psi_1|h^{ij}(t)|\psi_1\rangle$ for $t = 10$ to 20 is 0.0497 . For σ_z^1 the predicted equilibrium value is $2/14 \approx 0.143$, since the S_z subspace considered has 8 spins up and 6 spins down. The average value of $\langle\psi_2|h^{ij}(t)|\psi_2\rangle$ for $t = 10$ to 20 is 0.152 . For the integrable system the fluctuations around the long time average remains large even though the initial decays are of a similar form, consistent with the larger variance of diagonal matrix elements.

An interesting point to be made, is that for a chaotic system, since the frequency width of the envelope function does not depend on n , the convergence time to random state behavior, depends only on how many effective single and two qubit gates occur in a time interval. For a fixed Hamiltonian, the number of effective gates per time interval scales with the size of the system n . This corresponds precisely to the generic $1/n$ scaling per single and two qubit gates for convergence of moments of random quantum circuits. This, opens the question of whether a fixed chaotic Hamiltonian can be considered as approximating a "pseudo" t -design at a rate corresponding to the so-called Thouless time [76].

Chapter 8

Conclusions

We have shown that the convergence rate for t -order moments of reversible permutation invariant random quantum circuits scales as $\Gamma = a_t/n$ for sufficiently large n , where a_t may depend on t . Under the additional restriction of invariance under local gates, $a_t = a_2$ for all $t > 2$. We have additionally presented a random quantum circuit construction consisting of independently chosen single- and two-qubit gates that for $t = 2$ achieves the optimal asymptotic rate of $2/n$. Despite the fact that the asymptotic, large n rate does not depend on t , the border of the asymptotic region with respect to n is allowed to depend on t . Furthermore, the border to the asymptotic large n scaling must depend on t since polynomial length quantum circuits would otherwise be required to be dense in $U(N)$, which they are not. It is an important open problem to fully understand the simultaneous scaling of the convergence rate for moments of a random quantum circuit with respect to both t and n . Lastly, we have not considered the issue of robustness of random quantum circuits to noise, which is a necessary consideration for practical implementation of randomized algorithms. One interesting question is to determine the optimal circuit length for a random quantum circuit for a given error model, since each additional gate brings the circuit slightly closer to a random unitary transformation yet at the same time exposes the circuit to potential errors. Also, because a distribution is the target of a randomized circuit rather than a particular state of transformation, it is possible that a protocol employing a random quantum circuit is more robust against certain errors.

Quantum chaos is an interesting problem with several open areas of investigation. I have generalized the notion of Weyl laws that impose weak constraints on the statistics of eigenvectors of the Hamiltonian in the semi-classical limit of quantized versions of chaotic classical systems, to the case of non-integrable quantum many-body systems. The next logical step is to approach the fluctuations analytically, with discrete hops between states directly coupled by the Hamiltonian playing a similar role to periodic orbits in systems with a classical limit [38]. If the universal fluctuations can be rigorously shown to hold, or deviations from universality properly understood, then the approach to thermal equilibrium in quantum many-body systems can be put on a rigorous footing. Another line of investigation involves what distinctive dynamics chaotic quantum many-body systems may have, other than simply approaching equilibrium. Recent numerical results suggest that there is a rich phenomenology of dynamical regimes [86]. Furthermore, some effectively closed many-body quantum systems are potentially accessible to experimental investigation. Nuclear spin systems are particularly attractive since the long lattice relaxation times allow the system to be effectively closed on the time scale at which thermalization occurs. Some experimental results on long time relaxation are presented in [84]. Experiments have recently been performed in ultra-cold gases in optical lattices that suggest that thermal behavior in closed non-integrable quantum systems can be richer than its classical counterpart.

Lastly, we have presented evidence of the connection between the Thouless time of a chaotic many-body system and the rate at which a random quantum circuit approximates a 2-design. It may be fruitful to push the analogy further, continuing the formulation of a stochastic picture of many-body quantum chaos as begun in [85]. Specifically that the long time dynamics of a chaotic many-body system may be described in terms of a random walk over the unitary group. This suggests a natural connection between appropriately defined ensembles of random quantum circuits and pseudo-random time evolution induced by non-integrability that may be fruitful to explore.

Appendix A

Convergence Rates for Arbitrary Statistical Moments of Random Quantum Circuits

This appendix includes the following paper:

W. Brown, and L. Viola, “Convergence Rates for Arbitrary Statistical Moments of Random Quantum Circuits,” *Physical Review Letters* **104**, 250501 (2010).

Appendix B

Parameters of Pseudorandom Quantum Circuits

This appendix includes the following paper:

Y. Weinstein, W. Brown, and L. Viola, "Parameters of Pseudorandom Quantum Circuits," *Physical Review A* **78**, 052332 (2008).

Appendix C

Quantum Pseudorandomness from Cluster-State Quantum Computation

This appendix includes the following paper:

W. Brown, Y. Weinstein, and L. Viola, “Quantum Pseudorandomness from Cluster-State Quantum Computation,” *Physical Review A* **77**, 040303(R) (2008).

Appendix D

Chaos, Delocalization, and Entanglement in Disordered Heisenberg Models

This appendix includes the following paper:

W. Brown, L. Santos, D. Starling, and L. Viola “Quantum Chaos, Delocalization, and Entanglement in Disordered Heisenberg Models,” *Physical Review E* **77**, 021106 (2008).

Appendix E

Generalized Entanglement as a Framework for Complex Quantum Systems: Purity Versus Delocalization Measures

This appendix includes the following paper:

L. Viola and W. Brown, "Generalized Entanglement as a Framework for Complex Quantum Systems: Purity Versus Delocalization Measures," *Journal of Physics A: Mathematical and Theoretical* **40**, 8109 (2007).

Bibliography

- [1] C. Dankert, R. Cleve, J. Emerson, and E. Livine Phys. Rev. A **80**, 012304 (2009).
- [2] Y. Sekino and L. Susskind, J. High Energy Phys **10**, 065 (2008).
- [3] A. Bendersky, F. Pastawski, and J. P. Paz, Phys. Rev. A **80**, 032116 (2009).
- [4] E. Magesan, R. Blume-Kohout, and J. Emerson, arXiv:0910.1315.
- [5] J. Preskill and P. Hayden, J. High Energy Phys. **09**, 120 (2007).
- [6] M. B. Hastings, Nature Phys. **5**, 255 (2009).
- [7] A. W. Harrow and R. Low, Commun. Math. Phys. **291**, 257 (2009).
- [8] E. P. Wigner, Proc. Camb. Phil. Soc. **47**, 790 (1951).
- [9] J. B. French and V. K. B. Kota, Ann. Rev. Nucl. Part. Sci. **32**, 35 (1982).
- [10] Y. Elon, J. Phys. A **41**, 17 (2008).
- [11] J. Emerson, Y. S. Weinstein, M. Saraceno, S. Lloyd, and D. G. Cory, Science **302**, 2098 (2003).
- [12] J. Emerson, E. Livine, and S. Lloyd, Phys. Rev. A **72**, 060302 (2005).
- [13] J. Conway, *A Course in Functional Analysis* (Springer, New York, 1990).
- [14] C. W. Helstrom, *Quantum Detection and Estimation Theory* (Academic Press, New York, 1976).
- [15] A. Yu. Kitaev, A. H. Shen, and M. N. Vyalyi, *Classical and Quantum Computation* (American Mathematical Society, Boston, 2002).

- [16] R. Alicki and K. Lendi, *Quantum Dynamical Semigroups and Applications* (Springer, Berlin, 1987).
- [17] A. O. Barut and R. Raczyk, *Theory of Group Representations and Applications*, 3rd ed. (World Scientific, Singapore, 1986).
- [18] E. Wigner, Can. Math. Congr. Proc. (University of Toronto Press, Toronto, 174 (1957).
- [19] W. Brown and L. Viola, Phys. Rev. Lett. **104**, 250501 (2010).
- [20] W. G. Brown, Y. S. Weinstein, and L. Viola, Phys. Rev. A **77**, 040303(R) (2008).
- [21] J. P. Elliott and P. G. Dawber, *Symmetry in Physics*(Oxford University Press, New York, 1979), Vol. 2.
- [22] W. L. Spitzer and S. Star, Lett. Math. Phys. **63**, 165 (2003).
- [23] J. Kurmann, H. Thomas, and G. Mueller, Physica A **112**, 235 (1982).
- [24] S. M. Giampaolo, G. Adesso, and F. Illuminati, Phys. Rev. B **79**, 224434 (2009).
- [25] S. M. Giampaolo, G. Adesso, and F. Illuminati, Phys. Rev. Lett. **104**, 207202 (2010).
- [26] M. Carmer and J. Eisert, New J. Phys. **8**, 71 (2006).
- [27] H. L. Haselgrove, M. A. Nielsen, and T. J. Osborne, Phys.Rev.A **69**, 022301 (2004).
- [28] S. Okubo, J. Math. Phys. **16**, 528 (1975).
- [29] B. Kraus and J. I. Cirac, Phys. Rev. A **63**, 062309 (2001).
- [30] M. A. Nielsen and I. L. Chuang, *Quantum Information and Quantum Computation* (Cambridge University Press, Cambridge, 2000).
- [31] P. Diaconis, Proc. Natl. Acad. Sci. USA **93**, 1659 (1996).
- [32] R. Oliveira, O. C. Dahlsten, and M. B. Plenio, Phys. Rev. Lett. **98**, 130502 (2007).
- [33] O. C. Dahlsten, R. Oliveira, and M. B. Plenio, J. Phys. A **40**, 8081 (2007).

- [34] J. Rosenthal, *SIAM Review* **37**, 387 (1995).
- [35] R. Raussendorf and H. Briegel, *Phys. Rev. Lett.* **86**, 5188 (2001).
- [36] Y. S. Weinstein, W.G. Brown, and L. Viola, *Phys. Rev. A* **78**, 052332 (2008).
- [37] A. Peres *Quantum Theory: Concepts and Methods* (Kluwer, Dordrecht, 1993).
- [38] M. C. Gutzwiller, *Chaos in Classical and Quantum Mechanics* (Springer, New York, 1990).
- [39] P. Collet and J. Eckmann, *Concepts and Results in Chaotic Dynamics* (Springer, Berlin, 2006).
- [40] B. O. Koopman, *Proc. Nat. Acad. Sc.* **17**, 315 (1931).
- [41] R. Schack and C. M. Caves, *Phys. Rev. E* **53**, 3387 (1996).
- [42] R. Schack and C. M. Caves, *Phys. Rev. E* **53**, 3257 (1996).
- [43] C. M. Caves and R. Schack, *Complexity* **3**, 46 (1997).
- [44] T. Prosen, T. Seligman, and M. Znidaric, *Prog. Theor. Phys.* **150**, 200 (2003).
- [45] T. Gorin, T. Prosen, T. Seligman, and M. Znidaric, *Physics Reports* **435**, 33 (2006).
- [46] M. Rigol, V. Dunjko, and M. Olshanii, *Nature* **452**, 854 (2008).
- [47] M. Srednicki, *Phys. Rev. E* **50**, 888 (1994).
- [48] F. Haake, *Quantum Signatures of Chaos* (Springer, Berlin, 1991).
- [49] O. Bohigas, M. J. Giannoni, and C. Schmidt, *Phys. Rev. Lett.* **52**, 1 (1984).
- [50] U. Smilansky, *J. Phys. A* **40**, F621 (2007).
- [51] M. L. Mehta, *Random Matrices* (Elsevier, Amsterdam, 2004).
- [52] A. A. Terras, *IAS/Park City mathematical Series* **12**, 333 (2007).
- [53] J. P. Bouchaud and M. Potters, arXiv:q-fin:0910.1205 (2009).
- [54] S. Zelditch, *Commun. Math. Phys.* **160**, 81 (1994).

- [55] H. Weyl, *Math. Ann.* **141**, 441 (1912).
- [56] S. Zelditch, “Quantum ergodicity and mixing of eigenfunctions”, *Elsevier Encyclopedia of Mathematical Physics* (2005).
- [57] M. Feingold, N. Moiseyev, and A. Peres, *Chem. Phys. Lett.* **117**, 344 (1985).
- [58] M. Feingold and A. Peres, *Phys. Rev. A* **34**, 591 (1986).
- [59] A. H. Barnett, *Commun. Pure Appl. Math.* **59**, 1457 (2006).
- [60] A. Shnirelman, *Usp. Math. Nauk.* **29**, 181 (1974).
- [61] M. V. Berry, *J. Phys. A* **10**, 2083 (1977).
- [62] E. J. Heller, *J. Chem. Phys.* **72**, 1337 (1980).
- [63] E. J. Heller, *Chem. Phys. Lett.* **62**, 157 (1975).
- [64] O. Zariski and P. Samuel, *Commutative algebra* (Van Nostrand, New York, 1960).
- [65] P. Zanardi, *Phys. Rev. Lett.* **87**, 077901 (2001).
- [66] J. P. Blaizot and G. Ripka, *Quantum Theory of Finite Systems* (MIT Press, Cambridge, 1986).
- [67] R. Somma, H. Barnum, G. Ortiz, and E. Knill, *Phys. Rev. Lett.* **97**, 19 (2006).
- [68] F. Verstraete, J. I. Cirac, and V. Murg, *Adv. Phys.* **57**, 143 (2008).
- [69] T. A. Brody, J. Flores, J. B. French, P. A. Mello, A. Pandey, and S. S. M. Wong, *Rev. Mod. Phys.* **53**, 385 (1981).
- [70] V. Zelevinsky, *Ann. Rev. Nucl. Part. Sci.* **46**, 237 (1996).
- [71] V. K. B. Kota and R. Sahu, *Phys. Rev. E* **62**, 3569 (2000).
- [72] V. K. B. Kota, *Ann. Phys.* **306**, 58 (2003).
- [73] D. Greenbaum, *J. Magn. Reson.* **179**, 11 (2005).
- [74] R. Kubo, M. Toda and N. Hashitsume, *Statistical Physics II* (Springer-Verlag, Berlin, 1978).

- [75] T. Prosen, J. Phys. A **35**, L737 (2002).
- [76] D. J. Thouless, J. Phys. C **6**, L49 (1973).
- [77] C. Jarzynski, Phys. Rev. E **56**, 2254 (1997).
- [78] M. Ledoux, *The Concentration of Measure Phenomenon* (Mathematical Surveys and Monographs, American Mathematical Society **89**, 2001).
- [79] V. D. Milman and G. Schechtman, *Asymptotic Theory of Finite-Dimensional Normed Spaces* (Lecture Notes in Mathematics, Springer, Berlin, 1986), 140 Appendix V.
- [80] W. G. Brown, L. F. Santos, D. J. Starling, and L. Viola, Phys. Rev. E **77**, 021106 (2008).
- [81] L. Viola and W. Brown, J. Phys. A **40**, 8109 (2007).
- [82] D. A. Meyer and N. R. Wallach, J. Math. Phys. **43**, 4273 (2002).
- [83] H. Barnum, E. Knill, G. Ortiz, R. Somma, and L. Viola, Phys. Rev. Lett. **92**, 107902 (2004).
- [84] S. W. Morgan, B. V. Fine, and B. Saam, Phys. Rev. Lett. **101**, 067601 (2008).
- [85] M. Srednicki, J. Phys. A **32**, 1163 (1999).
- [86] M. C. Banuls, J. I. Cirac, and M. B. Hastings, arXiv:1007.3957.